Versão do arquivo anexado / Version of attached file:

Versão do Editor / Published Version

Mais informações no site da editora / Further information on publisher's website:

https://journals.aps.org/prc/abstract/10.1103/PhysRevC.109.065202

DOI: 10.1103/PhysRevC.109.065202

Direitos autorais / Publisher's copyright statement:

Systematic study of flow vector fluctuations in $\sqrt{s_{NN}} = 5.02$ TeV Pb-Pb collisions

S. Acharya *et al.**
(ALICE Collaboration)

Measurements of the p_T-dependent flow vector fluctuations in Pb–Pb collisions at $\sqrt{s_{NN}} = 5.02$ TeV using azimuthal correlations with the ALICE experiment at the Large Hadron Collider are presented. A four-particle correlation approach [ALICE Collaboration, Phys. Rev. C **107**, L051901 (2023)] is used to quantify the effects of flow angle and magnitude fluctuations separately. This paper extends previous studies to additional centrality intervals and provides measurements of the p_T-dependent flow vector fluctuations at $\sqrt{s_{NN}} = 5.02$ TeV with two-particle correlations. Significant p_T-dependent fluctuations of the $\vec{V}_2$ flow vector in Pb–Pb collisions are found across different centrality ranges, with the largest fluctuations of up to $\sim$15% being present in the 5% most central collisions. In parallel, no evidence of significant p_T-dependent fluctuations of $\vec{V}_3$ or $\vec{V}_4$ is found. Additionally, evidence of flow angle and magnitude fluctuations is observed with more than 5σ significance in central collisions. These observations in Pb–Pb collisions indicate where the classical picture of hydrodynamic modeling with a common symmetry plane breaks down. This has implications for hard probes at high p_T, which might be biased by p_T-dependent flow angle fluctuations of at least 23% in central collisions. Given the presented results, existing theoretical models should be reexamined to improve our understanding of initial conditions, quark–gluon plasma properties, and the dynamic evolution of the created system.

I. INTRODUCTION

Studies of ultrarelativistic heavy-ion collisions at the Relativistic Heavy Ion Collider (RHIC) and the Large Hadron Collider (LHC) have demonstrated the formation of a strongly interacting matter called quark–gluon plasma (QGP) [1–7]. The space–time evolution of the QGP is well described by relativistic viscous hydrodynamic models [8,9]. An observable consequence of the QGP creation in these collisions is the anisotropic flow in the plane transverse to the beam direction [10–16]. This anisotropy can be quantified by the Fourier decomposition of the distribution of the azimuthal angle of the final-state particles relative to the common symmetry planes [17],

$$\frac{d^3N}{dp_T d\eta d\varphi} = \frac{d^2N}{2\pi dp_T d\eta}$$
$$\times \left(1 + 2\sum_{n=1}^{\infty} v_n(p_T, \eta) \cos[n(\varphi - \Psi_n(p_T, \eta))]\right),$$
(1)

where φ is the azimuthal angle of the emitted particles. The $v_n(p_T, \eta)$ and $\Psi_n(p_T, \eta)$ are the magnitude and orientation of the nth-order flow vector $\vec{V}_n(p_T, \eta) = v_n(p_T, \eta)e^{in\Psi_n(p_T, \eta)}$, respectively, which may depend on the transverse momentum (p_T) and the pseudorapidity (η) of the particles. This flow vector is affected by the initial collision geometry, which is dominated by the shape of the overlap region in the transverse plane between the colliding nuclei [18]. The initial anisotropy, the magnitude and orientation of which is quantified by the eccentricities ϵ_n and corresponding participant planes Φ_n [19–21], respectively, is converted into final-state momentum anisotropy by the interactions among the constituents of the QGP. For a uniform nuclear matter distribution in the initial state, the various symmetry plane angles, Ψ_n, coincide with the reaction plane defined by the impact parameter and beam direction for $n \geqslant 1$ [17]. However, due to event-by-event fluctuations of the position of the nucleons inside the nuclei and of the partonic constituents inside the nucleon, the symmetry plane angles, Ψ_n, fluctuate around the reaction plane, leading to nonzero odd flow coefficients [19,22–24]. Nonzero and large values of flow coefficients have been observed at both RHIC [4–7] and the LHC [14–16,25–32]. The flow coefficients v_n and their event-by-event fluctuations serve as excellent probes for constraining the initial state of heavy-ion collisions and for quantifying some of the QGP properties, such as the transport coefficients [18,23,33–39].

The anisotropic flow coefficients can be measured in a p_T-differential way by assuming that the two-particle correlation factorizes into a product of two single-particle flow coefficients, each a function of the properties of only one of the particles. Keeping the terminology from dihadron correlation

*Full author list given at the end of the article.

measurements of $V_{n\Delta}$ [40–43], one particle is denoted as the associated (a) and the other particle is denoted the trigger (t). The associated and trigger particles are chosen from a variable and fixed p_T range, denoted p_T^a and p_T^t, respectively. Factorization of the two-particle correlation $V_{n\Delta}$ between the trigger and associated particles can be described as

$$V_{n\Delta}\left(p_T^a, p_T^t\right) = v_n\left(p_T^a\right) v_n\left(p_T^t\right), \qquad (2)$$

where the $v_n(p_T^a)$ and $v_n(p_T^t)$ are the flow coefficients for the associated and trigger particles with transverse momenta p_T^a and p_T^t, respectively. The factorization breaks down in hydrodynamic calculations due to the event-by-event fluctuations of the initial energy density of the heavy-ion collision [44,45]. The breakdown of factorization has been observed at the LHC in Pb–Pb collisions at $\sqrt{s_{NN}} = 2.76$ TeV and p–Pb collisions at $\sqrt{s_{NN}} = 5.02$ TeV [41,46,47]. This breakdown is directly related to the flow vector fluctuations in different kinematic regions. The flow vector may fluctuate as a function of p_T in both magnitude and angle [19,21]. As such, the flow angle, $\Psi_n(p_T)$, will "wander" around the common symmetry plane angle Ψ_n [44]. This, in turn, implies that the p_T-integrated flow magnitude, v_n, should be interpreted as the flow of particles with respect to an integrated symmetry plane determined with particles from a specific and typically wide p_T range. The p_T-dependent flow angles also contribute to breaking the factorization in Eq. (2), as the equality in Eq. (2) assumes a single common symmetry plane angle for all particles in an event.

The p_T-dependent flow fluctuations can be probed with the principal component analysis (PCA) [48–52], which can isolate subleading flow modes. The PCA has been successfully used to measure the event-by-event flow fluctuations [53] and the factorization breaking of two-particle correlations $V_{n\Delta}$ as a function of both p_T and pseudorapidity η [54]. The decorrelation effects measured in η provide insight into the longitudinal hydrodynamic evolution of the system created in heavy-ion collisions and go beyond the assumption of a boost-invariant system used in many theoretical models [47,55]. However, measurements with the PCA technique have yet to isolate the flow angle and flow magnitude fluctuations. In this paper the flow vector fluctuations are integrated over pseudorapidity and are only studied as a function of p_T.

The usual way of measuring the flow vector fluctuations is with observables constructed from two-particle correlations [44,45]. Such measurements have shown significant flow vector fluctuations in central Pb–Pb collisions [46,47]. However, such measurements do not allow quantifying the individual contributions of the flow angle and magnitude fluctuations to the total flow vector fluctuations. Hydrodynamic models have predicted that the fluctuations of Ψ_n constitute more than half of the overall flow vector fluctuations [44]. Observables constructed from four-particle correlations are necessary to cancel out contributions from the flow angle or magnitude. Such observables were first presented in Ref. [56] in selected centrality intervals and revealed significant flow angle and magnitude fluctuations in central Pb–Pb collisions. In this paper the study in Ref. [56] is extended to additional centrality intervals, and measurements of flow vector fluctuations with

two-particle correlations at a collision energy of $\sqrt{s_{NN}} = 5.02$ TeV are also presented.

The paper is structured as follows: Section II describes the method used to calculate the observables, while the experiment and data are described in Sec. III. The treatment of statistical and systematic uncertainties is covered in Sec. IV, and the results are presented in Sec. V. Finally, a summary is given in Sec. VI.

II. METHOD

The m-particle correlations are calculated with the generic framework [57], an algorithm that calculates multiparticle azimuthal correlations corrected for nonuniform azimuthal detector acceptance and nonuniform detector efficiency. The flow coefficients are defined from the Fourier expansion in Eq. (1),

$$\langle v_n \rangle = \langle \langle \cos n(\varphi - \Psi_n) \rangle \rangle, \qquad (3)$$

where the single set of brackets, $\langle \rangle$, denotes an average over events, while the double set of brackets, $\langle \langle \rangle \rangle$, denotes an average over both particles and events. The flow angles, Ψ_n, cannot be measured experimentally event-by-event, so the root-mean-square of the flow coefficients are calculated with two-particle correlations [58],

$$\langle v_n^2 \rangle = \langle \langle \cos n(\varphi_1 - \varphi_2) \rangle \rangle. \qquad (4)$$

The p_T dependence of the flow coefficient is usually studied with the differential flow coefficient $v_n\{2\}(p_T)$ [58]:

$$
\begin{aligned}
v_n\{2\}(p_T) &= \frac{\langle \langle \cos\left[n\left(\varphi_1^{POI} - \varphi_2\right)\right] \rangle \rangle}{\sqrt{\langle \langle \cos[n(\varphi_1 - \varphi_2)] \rangle \rangle}} \\
&= \frac{\langle v_n(p_T)\, v_n \cos[n(\Psi_n(p_T) - \Psi_n)] \rangle}{\sqrt{\langle v_n^2 \rangle}}. \qquad (5)
\end{aligned}
$$

The φ^{POI} and φ refer to the azimuthal angles of the particles of interest (POI) and reference flow particles. The p_T refers to the p_T of the POIs selected from narrow p_T ranges. The reference flow particles are chosen from a wide kinematic range, which should ideally be limited to a region dominated by collective behavior. The $\Psi_n(p_T)$ represents the p_T-differential symmetry plane angles at a specific p_T range, which might fluctuate around the reference symmetry plane angles Ψ_n. The effect of the difference between $\Psi_n(p_T)$ and Ψ_n, due to p_T-dependent flow angle fluctuations, is quantified by the cosine term $\langle \cos[n(\Psi_n(p_T) - \Psi_n)] \rangle$. The effects of the p_T-dependent flow coefficient fluctuations are observed when the factorization hypothesis is broken:

$$\langle v_n(p_T) v_n \rangle \neq \sqrt{\langle v_n(p_T)^2 \rangle} \sqrt{\langle v_n^2 \rangle}. \qquad (6)$$

Aside from the effects of the p_T-dependent fluctuations of the flow angle and the flow magnitude, $v_n\{2\}$ also has contributions from nonflow sources such as jets or resonance decays. Such sources provide a flow signal but are not associated with bulk particle production or correlated with the symmetry plane angles Ψ_n.

To account for these effects, another two-particle correlation was proposed in Ref. [44],

$$
\begin{aligned}
v_n[2](p_T) &= \sqrt{\left\langle\!\left\langle \cos\left[n\left(\varphi_1^{\text{POI}} - \varphi_2^{\text{POI}}\right)\right]\right\rangle\!\right\rangle} \\
&= \sqrt{\langle v_n(p_T)^2\rangle},
\end{aligned} \tag{7}
$$

that is not affected by fluctuations in the flow angle or flow coefficient, and it is less affected by nonflow effects than $v_n\{2\}$. The difference between $v_n\{2\}$ and $v_n[2]$ is that the former takes the reference flow from a wide kinematic range and the POIs from a small p_T interval, and the latter takes two POIs from the same narrow p_T range. Since $v_n[2]$ is not affected by the flow angle and flow magnitude fluctuations, the p_T-dependent flow vector fluctuations can be probed by taking the ratio of $v_n\{2\}$ and $v_n[2]$:

$$
\frac{v_n\{2\}}{v_n[2]} = \frac{\langle v_n(p_T)\, v_n \cos n[\Psi_n(p_T) - \Psi_n]\rangle}{\sqrt{\langle v_n(p_T)^2\rangle}\sqrt{\langle v_n^2\rangle}}. \tag{8}
$$

If the ratio $v_n\{2\}/v_n[2]$ is smaller than unity, it indicates the presence of p_T-dependent flow vector fluctuations.

Another way to study flow vector fluctuations is to examine the factorization of two-particle correlations from different transverse momentum regions. Factorization of two-particle correlations was observed to hold in some kinematical ranges in Refs. [29,31,41,59] but is shown not to hold in general in Ref. [45]. The factorization can be tested with the factorization ratio r_n [45]:

$$
\begin{aligned}
r_n &= \frac{V_{n\Delta}\left(p_T^a, p_T^t\right)}{\sqrt{V_{n\Delta}\left(p_T^a, p_T^a\right)V_{n\Delta}\left(p_T^t, p_T^t\right)}} \\
&= \frac{\langle v_n(p_T^a)v_n(p_T^t)\cos\left[n\left(\Psi_n(p_T^a) - \Psi_n(p_T^t)\right)\right]\rangle}{\sqrt{\langle v_n^2(p_T^a)\rangle\langle v_n^2(p_T^t)\rangle}},
\end{aligned} \tag{9}
$$

which is a particular case of the ratio shown in Eq. (8), obtained by taking particles from two different narrow p_T ranges. Most known sources of nonflow do not factorize at low p_T [60], so $r_n = 1$ does not always hold. In a system dominated by flow, with no or negligible nonflow effects, r_n is smaller than or equal to unity due to the Cauchy-Schwarz inequality [45]. The factorization holds when r_n equals unity, while r_n smaller than unity indicates the presence of p_T-dependent flow vector fluctuations. If the triggered particles are selected from a wide kinematic range (making them equivalent to the reference particles), then r_n becomes identical to $v_n\{2\}/v_n[2]$. In general, however, r_n provides information about the structure of the two-particle correlations for triggered and associated particles, probing the fluctuations of the flow vector at p_T^a and p_T^t. In contrast, the ratio $v_n\{2\}/v_n[2]$ includes the p_T-integrated information and probes the p_T-differential flow vector with respect to the p_T-integrated flow vector.

The ratio $v_n\{2\}/v_n[2]$ and the factorization ratio r_n carry information about the flow angle and magnitude fluctuations but cannot isolate both contributions. Thus, it is desirable to separate these two effects to quantify the contributions from each source.

The flow angle fluctuations are studied with the observable A_n^{f}, which aims to isolate the p_T-dependent fluctuations of the flow angle [56],

$$
\begin{aligned}
A_n^{\text{f}} &= \frac{\left\langle\!\left\langle \cos\left[n\left(\varphi_1^{\text{POI}} + \varphi_2^{\text{POI}} - \varphi_3 - \varphi_4\right)\right]\right\rangle\!\right\rangle}{\left\langle\!\left\langle \cos\left[n\left(\varphi_1^{\text{POI}} + \varphi_2 - \varphi_3^{\text{POI}} - \varphi_4\right)\right]\right\rangle\!\right\rangle} \\
&= \frac{\langle v_n(p_T)^2\, v_n^2 \cos 2n[\Psi_n(p_T) - \Psi_n]\rangle}{\langle v_n(p_T)^2 v_n^2\rangle} \\
&\simeq \langle\cos 2n[\Psi_n(p_T) - \Psi_n]\rangle_w,
\end{aligned} \tag{10}
$$

where the third equality holds if the nonflow contribution is approximately the same for the numerator and denominator. The w subscript denotes that A_n^{f} is a weighted average with each event having a weight of v_n^4 [61]. If the flow angle fluctuates as a function of p_T, then A_n^{f} will be smaller than unity. If there are no p_T-dependent fluctuations of the flow angle, then A_n^{f} is equal to unity. The A_n^{f} corresponds to the cosine term in Eq. (8) but with twice the angle. Only a lower limit of the single-flow-angle fluctuations, $\langle\cos n[\Psi_n(p_T) - \Psi_n]\rangle$, can be obtained with the trigonometric double-angle formula due to the event averaging

$$
\begin{aligned}
\sqrt{\frac{A_n^{\text{f}} + 1}{2}} &\simeq \sqrt{\langle\cos^2 n[\Psi_n(p_T) - \Psi_n]\rangle} \\
&\geqslant \langle\cos n[\Psi_n(p_T) - \Psi_n]\rangle.
\end{aligned} \tag{11}
$$

It is also possible to probe the upper limit on the two-particle flow magnitude fluctuations since it must correspond to the remaining fluctuations of the flow vector. The ratio with $v_n\{2\}/v_n[2]$ quantifies the upper limit of the first-moment flow magnitude fluctuations, since

$$
\begin{aligned}
&\frac{v_n\{2\}/v_n[2]}{\sqrt{\langle\cos^2 n[\Psi_n(p_T^a) - \Psi_n]\rangle}} \\
&\qquad\leqslant \frac{v_n\{2\}/v_n[2]}{\langle\cos n[\Psi_n(p_T^a) - \Psi_n]\rangle} \\
&\qquad= \frac{\langle v_n(p_T)\, v_n \cos n[\Psi_n(p_T) - \Psi_n]\rangle}{\sqrt{\langle v_n(p_T)^2\rangle}\sqrt{\langle v_n^2\rangle}\langle\cos n[\Psi_n(p_T) - \Psi_n]\rangle} \\
&\qquad\approx \frac{\langle v_n(p_T)\, v_n\rangle}{\sqrt{\langle v_n(p_T)^2\rangle}\sqrt{\langle v_n^2\rangle}}.
\end{aligned} \tag{12}
$$

The above equation provides an upper limit on the first-moment flow magnitude fluctuations, but an exact measurement of the second-moment flow magnitude fluctuations can be obtained by taking the ratio of the four-particle correlations with opposite signs on the azimuthal angle belonging to particles from the same kinematic region:

$$
\frac{\left\langle \cos n\left(\varphi_1^{\text{POI}} + \varphi_2 - \varphi_3^{\text{POI}} - \varphi_4\right)\right\rangle}{\left\langle \cos n\left(\varphi_1^{\text{POI}} - \varphi_3^{\text{POI}}\right)\right\rangle\langle\cos n(\varphi_2 - \varphi_4)\rangle} = \frac{\langle v_n^2(p_T)v_n^2\rangle}{\langle v_n^2(p_T)\rangle\langle v_n^2\rangle}. \tag{13}
$$

Considering the p_T-integrated $\langle v_n^4\rangle/\langle v_n^2\rangle^2$ as the baseline, deviations from such a baseline indicate the presence of p_T-dependent flow magnitude fluctuations. The expression in

Eq. (13) is therefore normalized with the baseline to obtain a double ratio correlator M_n^{f} for measuring the p_{T}-dependent flow magnitude fluctuations:

$$M_n^{\mathrm{f}} = \frac{\langle v_n^2(p_{\mathrm{T}}) v_n^2 \rangle / \langle v_n^2(p_{\mathrm{T}}) \rangle \langle v_n^2 \rangle}{\langle v_n^4 \rangle / \langle v_n^2 \rangle^2}. \tag{14}$$

Together, these observables, A_n^{f} and M_n^{f}, allow us to probe the flow angle and magnitude fluctuations separately and provide a quantification of both of them. Additionally, the limits extracted with the trigonometric formula are comparable with the previous methods of measuring p_{T}-dependent flow vector fluctuations [46].

III. EXPERIMENTAL SETUP AND DATA SAMPLE

ALICE [62] is a dedicated heavy-ion experiment at the LHC. One of its focuses is the study of the properties of the QGP. The central barrel of the ALICE detector is encased in a large solenoid magnet. The inner tracking system (ITS) [63] is the innermost detector in the ALICE experiment. Its primary function is to localize the primary vertex with a resolution better than $100 \,\mu$m, to reconstruct secondary vertices, and to track and identify low-momentum particles ($p_{\mathrm{T}} < 200 \,\mathrm{MeV}/c$). It also improves momentum and angle resolution for particles reconstructed by the time projection chamber (TPC) [64]. The TPC is the primary tracking detector in ALICE. It is optimized for high-resolution charged-particle momentum measurements ranging from several hundred MeV/c up to 100 GeV/c. In the TPC, a pseudorapidity coverage of $|\eta| < 0.8$ ensures maximal coverage without loss of efficiency at the TPC edges. Additionally, the TPC has full 2π coverage in the azimuthal direction. The V0 system [65] consists of two arrays, V0A and V0C, which cover the pseudorapidity ranges of $2.8 < \eta < 5.1$ and $-3.7 < \eta < -1.7$, respectively. It is designed to provide triggers for the experiment and to separate beam-beam interactions from the background, such as beam-gas interactions. It is also used to measure charged-particle multiplicity in the forward region, which is used to determine the centrality of nucleus-nucleus collisions [66].

The events are selected according to a minimum bias trigger criterion which requires at least two of the following [65]: (1) hits in the silicon pixel detector of the ITS, (2) a signal in V0A, and (3) a signal in the V0C, as well as a reconstructed primary vertex within ± 10 cm of the nominal interaction point along the beam axis. The centrality of the events is determined by the sum of V0 signal amplitude in the scintillator arrays V0A and V0C [66]. Pileup events refer to events that are contaminated by one or more out-of-bunch or in-bunch collisions occurring within the readout time of the TPC. Such contaminated events cannot be accurately assigned to a proper centrality interval. Pileup events are therefore rejected based either on the presence of multiple reconstructed vertices or on the correlations between the number of tracks measured in the TPC and the number of tracks reconstructed with relatively fast detectors such as the ITS and time-of-flight (TOF) [67]. This effect is most significant in central collisions due to the large multiplicity of the pileup events. In this paper,

54M Pb–Pb collisions at $\sqrt{s_{\mathrm{NN}}} = 5.02$ TeV measured in the 2015 data-taking period at the LHC pass the event selection criteria. Charged tracks are reconstructed using the ITS and the TPC. Tracks are selected with at least 70 TPC space points out of a maximum of 159 possible points and a χ^2 per degree of freedom of the track fit to TPC space points less than 4. Tracks are required to have at least one hit in the silixon pixel detector (SPD). Additionally, tracks must have a distance of closest approach (DCA) to the primary vertex of less than 2 cm in the longitudinal direction and a p_{T}-dependent selection in the transverse direction ranging from 0.2 cm at 0.2 GeV/c to 0.016 cm at 5 GeV/c. Finally, the charged tracks are taken from the kinematic range of $|\eta| < 0.8$, and the tracks used for reference particles are also within $0.2 < p_{\mathrm{T}}^{\mathrm{ref}} < 5.0$ GeV/c. The p_{T} range is selected to extend beyond the upper bound of validity for hydrodynamics (~ 3 GeV/c) as the flow angle and magnitude fluctuations may increase beyond this regime. Nonflow correlations are suppressed by requiring a pseudorapidity gap, $|\Delta\eta|$, greater than or equal to 0.8 between particles in the calculation of the flow coefficients with two-particle correlations, and a subevent method with no pseudorapidity gap is used in the calculation of four-particle correlations.

IV. STATISTICAL AND SYSTEMATIC UNCERTAINTIES

The statistical uncertainties of the measurements are estimated with the bootstrap method of random sampling with replacement [68]. Ten similarly sized subsamples are sampled uniformly from the entire event ensemble. From these ten subsamples, 1000 generated event samples are constructed by randomly selecting ten subsamples from the original ten subsamples with replacement, i.e., the same subsample can be selected multiple times. For each of the 1000 generated event ensembles, the observables are calculated as a weighted average, providing a distribution for each observable. The statistical uncertainty is then estimated from the variance of the distribution for a given observable, which should approach the actual distribution given a large enough sampling.

The systematic uncertainties of the measurements are evaluated by varying the event and track selection criteria and are shown in Table I. The systematic uncertainties related to the event selection are investigated by repeating the analysis using different detectors for the centrality determination, changing the selection on the position of the primary vertex along the beam direction $|V_z|$, testing different magnetic field polarities, and testing different pileup selections. The systematic uncertainty associated with the centrality determination (Cent. est.) is estimated by conducting the full analysis with the SPD as an alternative centrality estimator. It is negligible for most observables but contributes up to 2.4% for r_3. The systematic uncertainty related to different primary vertex position criteria ($|V_z|$) is studied by changing the criterion from $|V_z| < 10$ cm to $|V_z| < 7$ cm, 8 cm, and 9 cm and is found to contribute at most up to 0.6% for r_3. The effects of the magnetic field polarity (Mag. Field) are tested by analyzing datasets with different magnetic configurations and yield a systematic uncertainty ranging from negligible and up to 2.4% for $v_4\{2\}/v_4[2]$. The systematic effect of pileup is estimated by changing the pileup

TABLE I. Systematic uncertainties estimated from variations of event and track selection criteria. The uncertainties may vary with centrality and are, in those cases, given as a lower and upper bounds. Systematic uncertainties that are not statistically significant are listed as N/S. See text for details.

	$v_2\{2\}/v_2[2]$	$v_3\{2\}/v_3[2]$	$v_4\{2\}/v_4[2]$	r_2	r_3	A_2^{f}	M_2^{f}
Cent. est.	N/S	0%–0.2%	0%–0.7%	0%–0.3%	0%–2.4%	0%–0.1%	0%–0.1%
$\lvert V_z \rvert$	N/S	N/S	N/S	0%–0.1%	0%–0.6%	0%–0.1%	0%–0.1%
Mag. field	0%–0.1%	0.1%–1%	0%–2.4%	0%–0.5%	0%–2%	0.4%	0.4%
Pileup	N/S	0%–0.3%	0%–1.2%	0%–0.5%	0%–1.1%	N/S	N/S
# TPC cls.	N/S	N/S	0%–0.7%	0%–2%	0%–2%	0.7%	0.7%
Track type	0%–0.2%	0.5%–1.3%	1.1%–2.2%	0%–1.8%	0%–1.3%	0%–0.1%	0%–0.1%
$\lvert \mathrm{DCA}_z \rvert$	N/S	N/S	N/S	N/S	N/S	N/S	N/S
$\lvert \mathrm{DCA}_{xy} \rvert$	N/S	0%–1%	N/S	N/S	0%–1%	0%–0.1%	0%–0.1%
χ^2 TPC cls.	0%–0.1%	0%–0.3%	0%–3.1%	0%–0.8%	0%–0.5%	0.4%	0.4%
Nonflow	0%–0.6%	0.6%–1.7%	2%–3.4%	0.1%–2.3%	0%–5.9%	1.1%	1.1%

selection in centrality interval 0–10% (Pileup), where the pileup events are expected to have the largest impact due to large multiplicities in the TPC. The pileup selection variation contribution to the systematic uncertainty ranges from negligible to at most ∼1% for r_3 and $v_4\{2\}/v_4[2]$.

The quality of the reconstructed tracks is varied by changing the track type to include tracks without hits in the SPD (track type) and by modifying the minimum number of TPC space points required (# TPC cls.) from 70 to 80 and 90. This variation yields up to a 2% systematic uncertainty in the r_n observables and less than 1% in the other observables. Additionally, the requirement of maximum DCA in the longitudinal (z) direction ($\lvert \mathrm{DCA}_z \rvert$) is changed from 2 cm to 0.5 and 1 cm, and in the transverse (xy) direction ($\lvert \mathrm{DCA}_{xy} \rvert$) it is changed from a p_{T}-dependent selection ($\lvert \mathrm{DCA}_{xy} \rvert \leqslant N_\sigma \times (0.0015 + 0.005/p_{\mathrm{T}}^{1.1})$) corresponding to 7σ deviation from the expected functional form to one corresponding to 4σ. Both variations of the $\lvert \mathrm{DCA}_z \rvert$ and the variation of $\lvert \mathrm{DCA}_{xy} \rvert$ selection criteria yield negligible contributions to the systematic uncertainty for most of the observables. The last variation considered for the track quality is the χ^2 per TPC cluster (χ^2 TPC cls.), which is tightened from 4 to 2.5 and yields a systematic uncertainty of up to 3.1% for $v_4\{2\}/v_4[2]$ but less than half a percent for the other observables. To estimate the systematic uncertainty associated with the nonflow suppression in two-particle correlations (Non-flow), the analysis is repeated with pseudorapidity gaps of $\lvert \Delta\eta \rvert < 0.6, 1.0, 1.2$. The consistency between results with different pseudorapidity gaps suggests that short-range nonflow correlations are suppressed. It is possible that remaining long-range nonflow correlations such as those from momentum conservation and di-jets could influence the results, even though an additional Monte Carlo study with HIJING [69], a heavy-ion model that does not contain collective effects, showed results for the correlators in Eqs. (10) and (12) consistent with zero. Based on the above studies, it is found that the remaining nonflow contribution to the observables is less than ∼2% for the elliptic flow observables. The systematic uncertainty is estimated for each centrality interval separately (and additionally for each $p_{\mathrm{T}}^{\mathrm{t}}$ range for the calculation of r_n). The statistical significance of the systematic uncertainty is evaluated with the Barlow check introduced in Ref. [70]. Only systematic uncertainties

found to be statistically significant according to this check are considered for the final systematic uncertainty. The total systematic uncertainty is calculated as the quadratic sum of the individual sources. Only the variation resulting in the largest uncertainty is added to the total systematic uncertainty for sources with more than one variation.

V. RESULTS

In this paper, precision measurements of the ratio $v_n\{2\}/v_n[2]$ are presented for $n = 2, 3$ and 4 in Pb–Pb collisions at $\sqrt{s_{\mathrm{NN}}} = 5.02$ TeV. The results are compared with the existing measurements at $\sqrt{s_{\mathrm{NN}}} = 2.76$ TeV. Figure 1 shows the ratio $v_2\{2\}/v_2[2]$ with $\lvert \Delta\eta \rvert > 0.8$ as a function of p_{T} for various centrality intervals ranging from 0%–5% up to 40%–50%. For the most central collisions (0%–5%), the ratio for $n = 2$ is consistent with unity up to $p_{\mathrm{T}} \approx 2$ GeV/c. It starts to deviate from unity as the p_{T} increases with a significance higher than 2σ, 3σ, and 5σ in the three bins above 2 GeV/c, respectively. The ratio reaches a deviation of 15% from unity at $p_{\mathrm{T}} > 3$ GeV/c. For centrality intervals larger than 20%, the ratios are close to unity within 2% for the presented p_{T} range. This trend was already observed with measurements based on ALICE data at $\sqrt{s_{\mathrm{NN}}} = 2.76$ GeV/c [46]. The data are compared to several theoretical models. The iEBE-VISHNU model is a (2+1)D event-by-event relativistic viscous hydrodynamic model coupled to a hadronic cascade model [72]. In this paper, two sets of calculations with the iEBE-VISHNU model are used: one with T_RENTo [73] and one with AMPT [74] initial conditions. The model calculations with T_RENTo initial conditions use a temperature-dependent specific shear viscosity $\eta/s(T)$, while the calculations with AMPT initial conditions use a $\eta/s = 0.08$. The input parameters of iEBE-VISHNU are tuned according to [71]. The hydrodynamic calculations are performed in a p_{T} range up to 3 GeV/c, as this is the region where hard processes are expected to take over.

The theory curves describe quantitatively $v_2\{2\}/v_2[2]$ within the uncertainties for both sets of model calculations. The large uncertainties of the hydrodynamic calculations are due to limited number of produced Monte Carlo events.
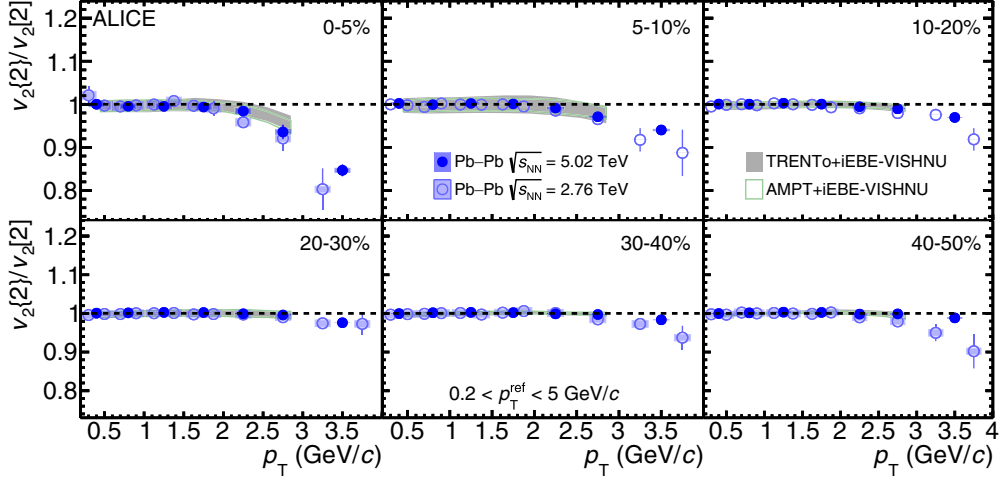
FIG. 1. The ratio $v_2\{2\}/v_2[2]$ in Pb–Pb collisions at $\sqrt{s_{NN}} = 5.02$ TeV (solid dark blue circles) and 2.76 TeV [46] (open light blue circles) as a function of transverse momentum. The different panels display results in different centrality intervals. Statistical (systematic) uncertainties are represented by solid bars (faded boxes). Predictions from the iEBE-VISHNU hydrodynamic model with T_RENTo initial conditions and temperature-dependent $\eta/s(T)$ [71], and with AMPT initial conditions and $\eta/s = 0.08$ [71], are shown in colored bands.

Higher-order anisotropic flow measurements were measured for the first time in Ref. [25] and were found to be more sensitive to the initial conditions and properties of the QGP [22]. The ratio $v_3\{2\}/v_3[2]$ with $|\Delta\eta| > 0.8$ is shown in Fig. 2. It can be seen that the ratio agrees with unity in the presented centrality and p_T ranges, unlike $v_2\{2\}/v_2[2]$, as shown in Fig. 1. The agreement with unity suggests that the triangular flow vector $\vec{V}_3$ does not fluctuate strongly with p_T in the presented p_T and centrality ranges. Previously published measurements [46] have substantial uncertainties for $v_3\{2\}/v_3[2]$ and found no significant $\vec{V}_3$ fluctuations. With these results, the findings in Ref. [46] are confirmed with substantially increased statistics, and it can be concluded that there are no significant p_T-dependent $\vec{V}_3$ fluctuations in Pb–Pb collisions at $\sqrt{s_{NN}} = 5.02$ TeV within the current

experimental uncertainties. The hydrodynamic calculations with the iEBE-VISHNU hydrodynamic models describe the data. The models with T_RENTo and AMPT initial conditions show agreement with unity and the data. At small p_T in central collisions, the hydrodynamical calculations deviate slightly from unity and overestimate the effect of the flow vector fluctuations observed in the data.

The ratio $v_4\{2\}/v_4[2]$ with $|\Delta\eta| > 0.8$ shown in Fig. 3 is consistent with unity within the uncertainties across all centrality intervals. The previous measurements of $v_4\{2\}/v_4[2]$ [46] had large statistical uncertainties and showed no statistically significant deviation from unity. The results presented in this paper do not show any sign of significant fluctuations of $\vec{V}_4$ as a function of transverse momentum with significantly smaller uncertainties compared to the measurements in
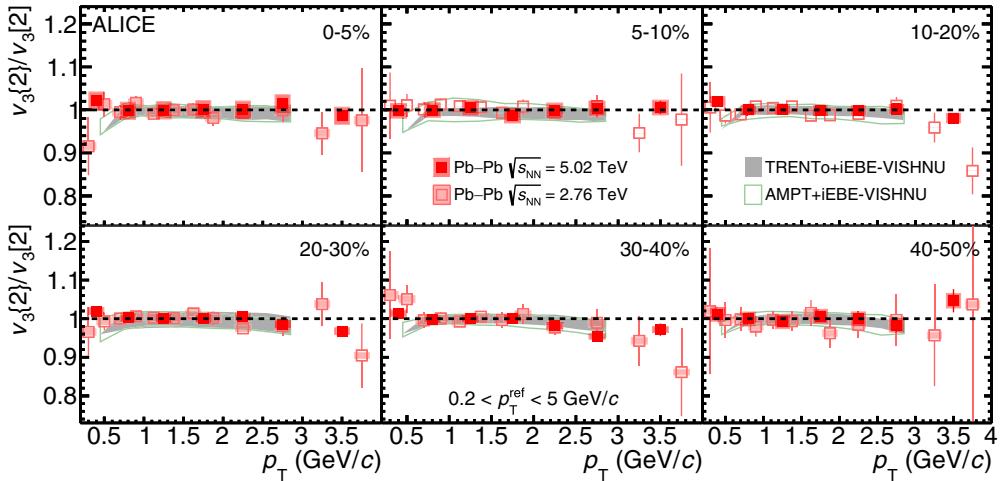

FIG. 2. The ratio $v_3\{2\}/v_3[2]$ for Pb–Pb collisions at $\sqrt{s_{NN}} = 5.02$ TeV (solid dark red squares) and 2.76 TeV [46] (open light red squares) as a function of transverse momentum. The different panels display results in different centrality intervals. Statistical (systematic) uncertainties are represented by solid bars (faded boxes). Predictions from iEBE-VISHNU hydrodynamic model with T_RENTo initial conditions and temperature-dependent $\eta/s(T)$ [71], and with AMPT initial conditions and $\eta/s = 0.08$ [71], are shown in colored bands.
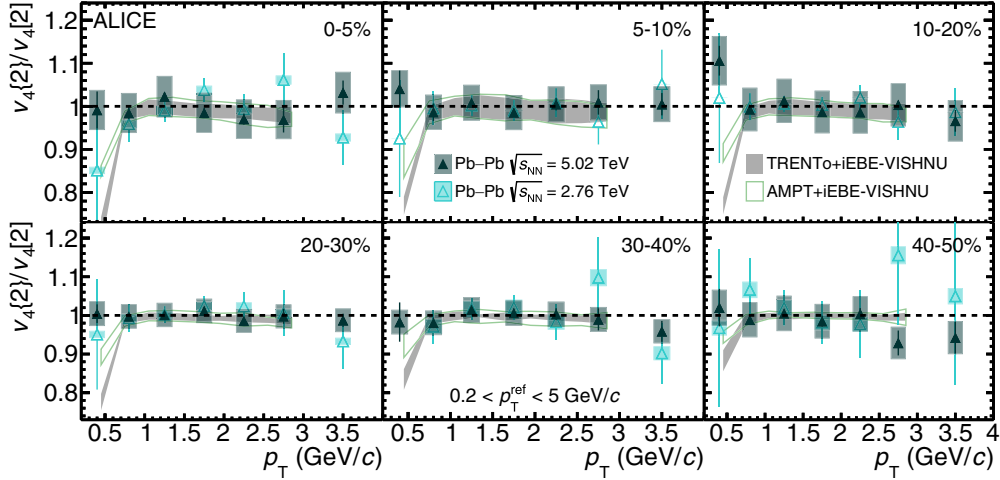
FIG. 3. The ratio $v_4\{2\}/v_4[2]$ for Pb–Pb collisions at $\sqrt{s_{NN}} = 5.02$ TeV (solid dark cyan triangles) and 2.76 TeV [46] (open light cyan triangles) as a function of transverse momentum. The different panels display results in different centrality intervals. Statistical (systematic) uncertainties are represented by solid bars (faded boxes). Comparison with iEBE-VISHNU hydrodynamic model with T_RENTo initial conditions and temperature-dependent $\eta/s(T)$ [71], and with AMPT initial conditions and $\eta/s = 0.08$ [71], are shown in colored bands.

Ref. [46]. The hydrodynamic calculations are consistent with unity for $p_T > 0.6$ GeV/c but show a deviation from unity at low p_T inconsistent with the measured $v_4\{2\}/v_4[2]$.

This paper also presents precision measurements of the factorization ratios r_n in Pb–Pb collisions at $\sqrt{s_{NN}} = 5.02$ TeV for $n = 2$ and 3, calculated according to Eq. (9). Figure 4 shows r_2 with a pseudorapidity gap $|\Delta\eta| > 0.8$ as a function of p_T^a in centrality intervals 0%–5%, 10%–20%, and 40%–50% in various bins of p_T^t. For all p_T^t bins, it is observed that the deviations from unity are largest in central collisions, where the initial-state geometry fluctuations dominate, and that the effect becomes more pronounced as the difference $|p_T^a - p_T^t|$ increases. The largest deviations from unity are observed in central collisions for $0.2 < p_T^t < 0.6$ GeV/c with $3.0 < p_T^a < 4.0$ GeV/c (first row, left panel) and for $3.0 < p_T^t < 4.0$ GeV/c with $0.2 < p_T^a < 0.6$ GeV/c (last row, left panel), since this is the momentum region where the difference $|p_T^a - p_T^t|$ is the largest. For 40%–50% centrality, the deviation from unity is at most 3% across the different p_T^t ranges. The factorization is broken in central collisions, which, in turn, implies the presence of p_T-dependent flow vector fluctuations as described in Ref. [45]. At a higher p_T^t, the deviations from unity become less pronounced since the difference $|p_T^a - p_T^t|$ reaches the largest value in the lowest p_T^t bin. Significant deviations of r_2 from unity have been measured at lower energy [46] and confirmed here in Pb–Pb collisions at $\sqrt{s_{NN}} = 5.02$ TeV. Compared with previous results, the precision of r_2 is drastically improved, with the deviations from unity being significant to more than 5σ at $3.0 < p_T^a < 4.0$ GeV/c across the presented centralities.

The centrality dependence of r_2 is more clearly seen in Fig. 5, where r_2 is presented in the centrality intervals 0%–5% to 40%–50% in the lowest p_T bin of $0.2 < p_T < 0.6$ GeV/c. The comparison with the hydrodynamic calculations from iEBE-VISHNU with AMPT and T_RENTo initial conditions is presented. Both hydrodynamic calculations qualitatively describe the trend of r_2. However, they also underestimate the

deviations from unity at higher p_T in central collisions. The hydrodynamic model with AMPT initial conditions produces a slightly larger deviation of r_2 from unity at $p_T > 2.5$ GeV/c in central collisions than the one with T_RENTo initial conditions, while both provide a reasonable description of the data in peripheral collisions.

Figure 6 shows r_3 with $|\Delta\eta| > 0.8$ as a function of p_T^a for different bins of p_T^t, and in centrality intervals 0%–5%, 10%–20% and 40%–50%. Here, r_3 is consistent with unity in the presented centralities and p_T^a range for all p_T^t. The agreement with unity over the presented centrality range suggests no significant $\vec{V}_3$ fluctuations independently of the centrality. The lack of a centrality dependence agrees with the picture that triangular flow is driven by initial-state fluctuations rather than the average geometry. The factorization is also observed to hold over the presented ranges of p_T^a and p_T^t, as opposed to r_2. The previous measurements [46] showed deviations from unity at high p_T in several bins of p_T^t but without a large significance (less than 3σ). It was noted that a possible breakdown of the factorization would be within 10% when both p_T^a and p_T^t are below 3 GeV/c. The precision measurements presented in this paper lowers the possible breakdown of factorization of the triangular flow, v_3, down to 1% across the presented p_T and centrality ranges within a 95% confidence interval.

The measurements of the p_T-dependent flow angle fluctuations A_2^f are shown in Fig. 7 as a function of the transverse momentum p_T in centrality intervals 0%–5% to 40%–50%. More than a 5σ significance is observed in all centralities for the flow angle fluctuations at the highest p_T values. A deviation from unity of up to 23% is observed in the 5% most central collisions for the highest p_T value with a significance of 13σ. The strength of the fluctuations decreases towards more peripheral collisions to around 5% in 20%–30% and 30%–40% and then slightly increases in 40%–50% centrality up to 7%. These measurements provide evidence of p_T-dependent flow angle fluctuations. As the systematic uncertainty accounts for any potential remaining nonflow
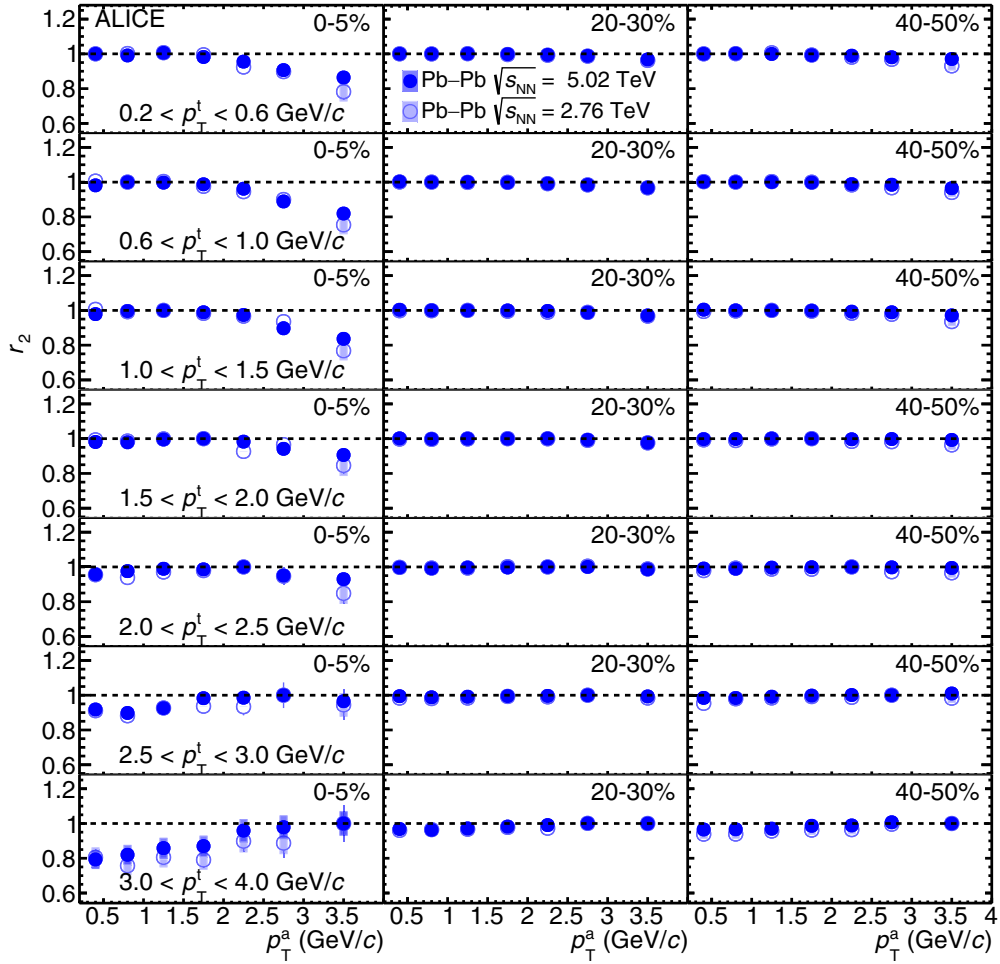
FIG. 4. The factorization ratio r_2 for Pb–Pb collisions at $\sqrt{s_{NN}} = 5.02$ TeV (dark blue circles) and 2.76 TeV [46] (light blue circles) as a function of associated particle p_T^a. The columns show the results in centrality intervals 0%–5%, 20%–30%, and 40%–50%, while the rows show the results for different trigger particle p_T^t intervals. Statistical (systematic) uncertainties are represented by solid bars (faded boxes).
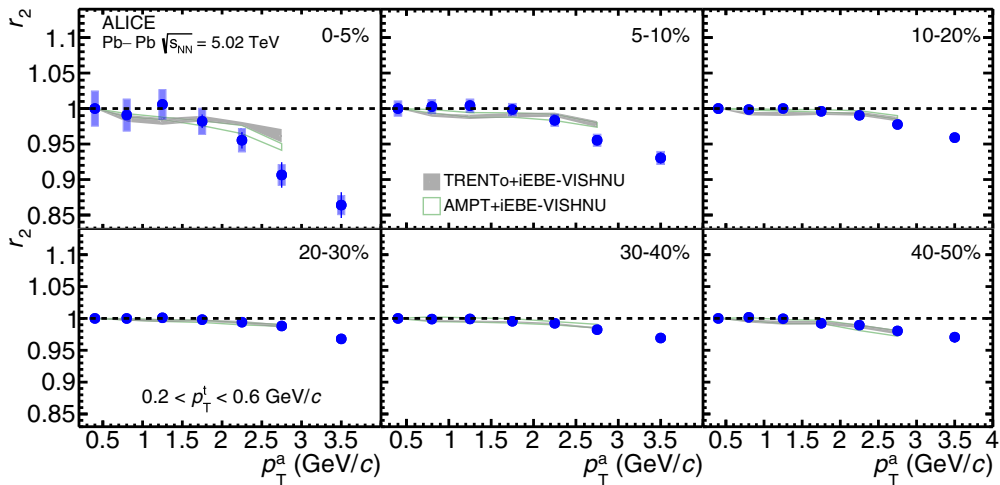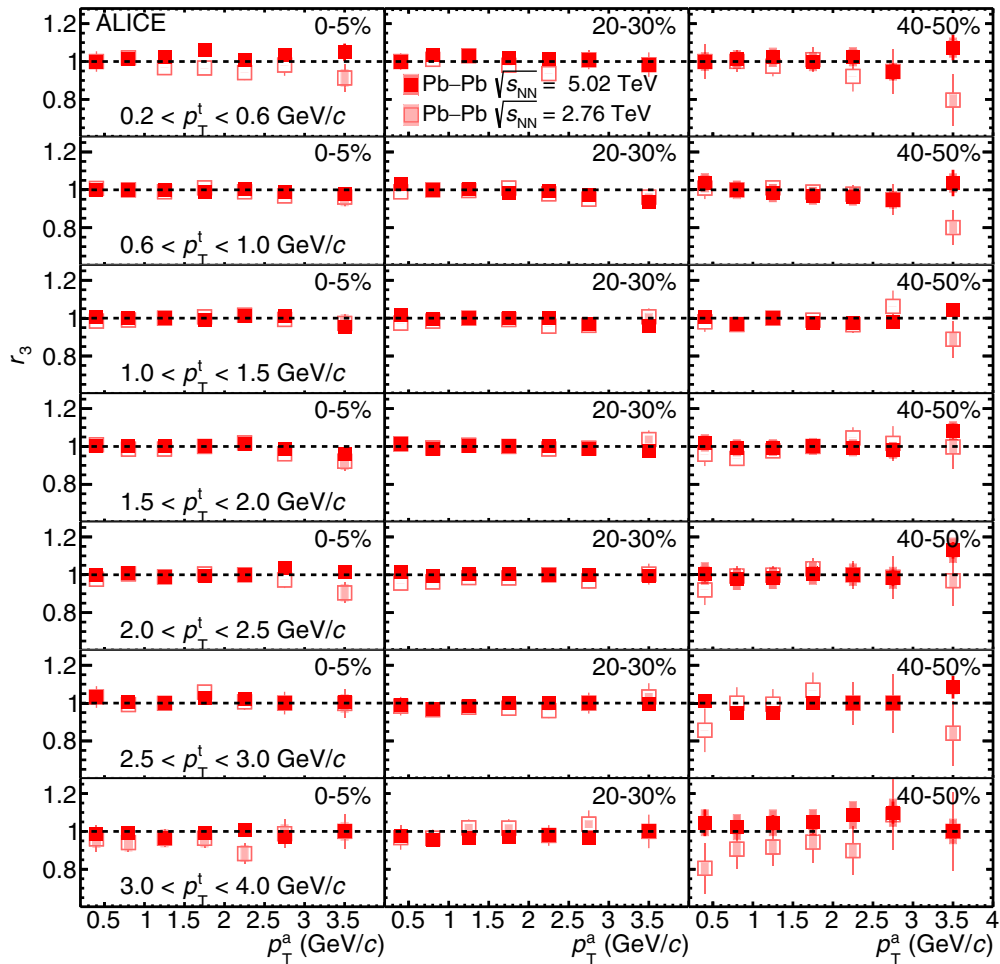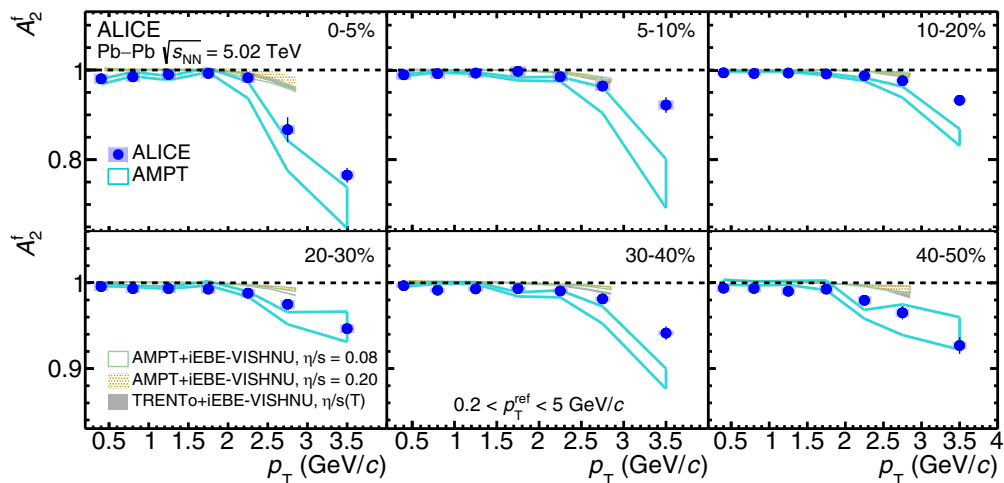

FIG. 5. The factorization ratio r_2 for Pb–Pb collisions at $\sqrt{s_{NN}} = 5.02$ TeV (blue circles) as a function of p_T^a for $0.2 < p_T^t < 0.6$ GeV/c. The different panels display results in different centrality intervals. Statistical (systematic) uncertainties are represented by solid bars (faded boxes). Predictions from iEBE-VISHNU hydrodynamic model with T$_R$ENTo initial conditions and temperature-dependent $\eta/s(T)$ [71], and with AMPT initial conditions and $\eta/s = 0.08$ [71], are shown in colored bands.

FIG. 6. The factorization ratio r_3 in Pb–Pb collisions at $\sqrt{s_{NN}} = 5.02$ TeV (solid dark red squares) and 2.76 TeV [46] (open light red squares) as a function of p_T^a. The columns show the results in centrality intervals 0%–5%, 20%–30%, and 40%–50%, while the rows show the results for different trigger particle p_T^t intervals. Statistical (systematic) uncertainties are represented by solid bars (faded boxes).

FIG. 7. The flow angle fluctuations A_2^f in Pb–Pb collisions at $\sqrt{s_{NN}} = 5.02$ TeV (blue circles) as a function of p_T. The different panels display results in different centrality intervals. Statistical (systematic) uncertainties are represented by solid bars (faded boxes). Predictions from iEBE-VISHNU with AMPT initial conditions and $\eta/s = 0.08$, 0.20 and iEBE-VISHNU with T$_R$ENTo initial conditions and $\eta/s(T)$ [71] as well as AMPT [74] are shown in colored bands.
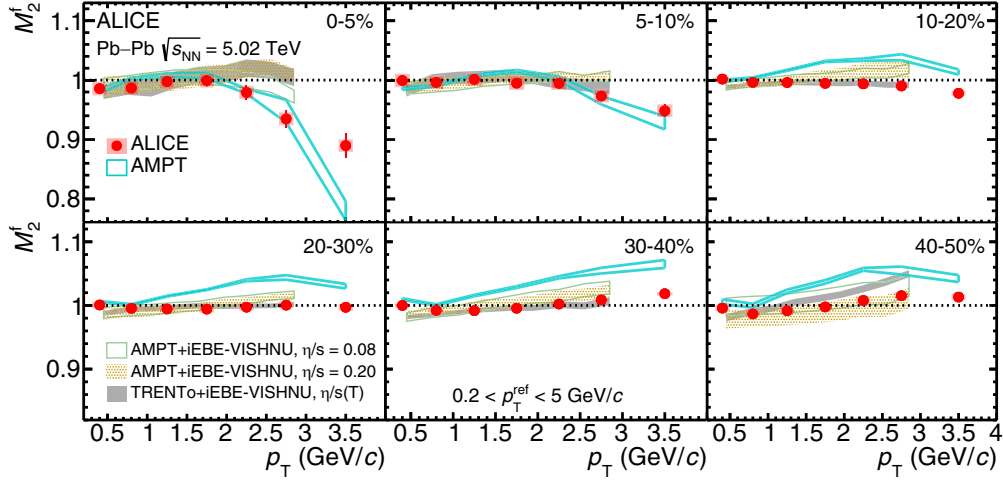
FIG. 8. The flow magnitude fluctuations M_2^{f} in Pb–Pb collisions at $\sqrt{s_{\mathrm{NN}}} = 5.02$ TeV (red squares) as a function of p_{T}. The different panels display results in different centrality intervals. Statistical (systematic) uncertainties are represented by solid bars (faded boxes). Predictions from iEBE-VISHNU with AMPT initial conditions and $\eta/s = 0.08$, 0.20 and iEBE-VISHNU with $\mathrm{T_R}$ENTo initial conditions and $\eta/s(T)$ [71] as well as AMPT [74] are shown in colored bands.

contributions, it is clear that they cannot explain the deviation of A_2^{f} from unity. Large fluctuations in central collisions are expected since the collisions are dominated by event-by-event fluctuations in the position of the nucleons and of the quarks and gluons within the nucleons. For the more peripheral events, the pressure gradients due to the geometric anisotropy of the overlap region between the colliding nuclei dominate, decreasing the flow angle fluctuations. The comparison with hydrodynamic calculations shows that iEBE-VISHNU model underestimates the effects of the flow angle fluctuations at $p_{\mathrm{T}} > 2.5$ GeV/c. The $\mathrm{T_R}$ENTo +iEBE-VISHNU with temperature-dependent shear viscosity to entropy density ratio $\eta/s(T)$ and AMPT+iEBE-VISHNU with $\eta/s = 0.08$ show around 5% (4%) deviation from unity with a significance of 7σ (9σ) in the 0%–5% central collisions compared to AMPT+iEBE-VISHNU with $\eta/s = 0.20$, which predicts around 2% deviation from unity with 2.7σ significance. However, none of the hydrodynamic models succeeds in quantitatively describing the large measured flow angle fluctuations at high p_{T} in the 0%–5% central collisions. The AMPT transport model calculations quantitatively predict the flow angle fluctuations in the 0%–5% most central collisions and the 20%–30% and 40%–50% centrality intervals but overestimate the deviation in the other centrality intervals.

Figure 8 shows the measurements of M_2^{f} as a function of the transverse momentum p_{T} in centrality intervals 0%–5% to 40%–50%. Similarly to the flow angle fluctuations, a significant deviation from unity is observed in the 0%–5% most central collisions with values up to $\sim$12%. As the centrality increases to 20%–30%, the flow magnitude fluctuations become smaller. Towards more peripheral collisions, M_2^{f} becomes larger than unity. In two-particle correlations, the values of ratios such as $v_n\{2\}/v_n[2]$ and r_n are strictly less than unity due to the Cauchy-Schwarz inequality. However, by construction, M_2^{f} does not satisfy this inequality and so values can exceed unity. The comparison with theoretical predictions shows that iEBE-VISHNU with $\mathrm{T_R}$ENTo initial conditions

and AMPT initial conditions underestimate the deviations in the most central collisions. At higher centralities the model calculations are consistent with the data and correctly describe the modestly increasing trend in the data in 30%–40% and 40%–50% centrality intervals. The comparison of the AMPT+iEBE-VISHNU hydrodynamic calculations with different η/s show some difference in the 5% most central collisions. Such a dependence of M_2^{f} on η/s in hydrodynamic models was also seen in Ref. [56], while further AMPT model calculations [75] suggest that M_2^{f} is not very sensitive to the value of η/s. This should be investigated with further model studies. Pure AMPT calculations accurately describe the deviation from unity in the 0%–5% and 5%–10% most central collisions but fail to reproduce the data at higher centralities.

In Fig. 9 the lower limit of the flow angle fluctuations [see Eq. (11)], the upper limit of the flow magnitude fluctuations [see Eq. (12)], and the flow vector fluctuations [see Eq. (8)] are shown as a function of transverse momentum in centrality intervals 0%–5% to 40%–50%. The figure shows the limits of the single flow angle and first-moment flow magnitude fluctuations, which are the factors of the total flow vector fluctuations measured by $v_n\{2\}/v_n[2]$. While the exact contribution of the single-angle flow angle fluctuations and the first-moment flow magnitude fluctuations cannot be established, information about the fluctuations can still be inferred from the limits. The flow angle fluctuations contribute at least $\sim$40% to the total flow vector fluctuations measured with $v_2\{2\}/v_2[2]$ in 0%–5% central collisions, and it also contributes at higher centralities, where all the sources of fluctuations decrease. This effect is consistent with the measured A_2^{f} and with what has been predicted by hydrodynamic calculations [44]. At centralities above 30%, the first moments of the flow magnitude fluctuations vanish, as the upper limit of the flow magnitude fluctuations, denoted by the red squares in Fig. 9, converges towards the lower limit of unity (with unity implying no fluctuations). The disappearance of the flow magnitude fluctuations indicates that above 30% centrality,
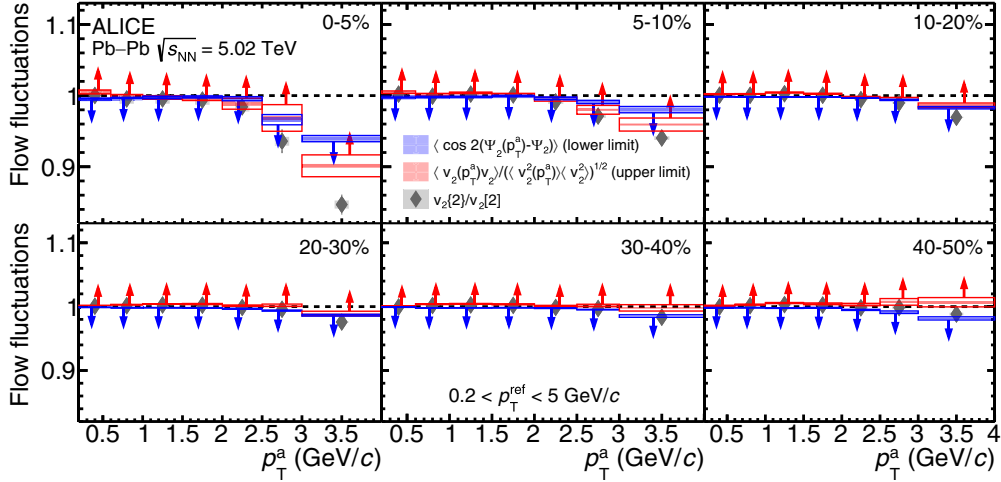
FIG. 9. The lower limit of $\langle \cos n(\Psi_2(p_T) - \Psi_2) \rangle$ (blue boxes), the upper limit of $\langle v_2(p_T)v_2 \rangle / \sqrt{\langle v_2^2(p_T) \rangle \langle v_2^2 \rangle}$ (red boxes), and the flow vector fluctuations $v_2\{2\}/v_2[2]$ (gray diamonds) as a function of p_T. The different panels display results in different centrality intervals. The red (blue) arrows denote the upper (lower) limits, and the statistical (systematic) uncertainties are represented by open (shaded) boxes.

the flow vector fluctuations are solely due to or dominated by fluctuations of the flow angle. For M_2^f, i.e., the second-moment flow magnitude fluctuations, this is not the case, as deviations from unity, although small, are observed at all centralities.

VI. SUMMARY

Measurements of the p_T-dependent flow vector fluctuations in Pb–Pb collisions at $\sqrt{s_{NN}} = 5.02$ TeV with the ratio $v_n\{2\}/v_n[2]$ up to $n = 4$, and the factorization ratio r_n up to $n = 3$ are presented. Deviations of both $v_2\{2\}/v_2[2]$ and r_2 from unity suggest the presence of p_T-dependent $\vec{V}_2$ fluctuations. The p_T-dependent fluctuations of $\vec{V}_2$ reach ~15% in central collisions for $v_2\{2\}/v_2[2]$ at high p_T as well as for r_2 when $|p_T^a - p_T^t|$ is large. The p_T-dependent flow vector fluctuations of $\vec{V}_3$ and $\vec{V}_4$ measured via $v_n\{2\}/v_n[2]$ ($n = 3, 4$) and r_n ($n = 3$) are within a few percent. The $v_n\{2\}/v_n[2]$ and r_n results are consistent with previous measurements in Pb–Pb collisions at $\sqrt{s_{NN}} = 2.76$ TeV [46,47] but offer significantly better precision. Comparison with the iEBE-VISHNU hydrodynamic model shows that the model with AMPT initial conditions and $\eta/s = 0.08$ [71] or T$_R$ENTo initial conditions and temperature-dependent $\eta/s(T)$ describe flow vector fluctuations well across the presented centrality ranges.

The contributions of flow angle and magnitude fluctuations are separated from the overll flow vector fluctuations with the proposed correlators A_n^f and M_n^f in various centrality intervals from 0%–50%. Fluctuations of the flow angle and magnitude are observed at higher values of p_T, with the largest fluctuations observed in 0%–5% central collisions. This observation is consistent with the flow vector fluctuations measured with two-particle correlations, exhibiting the largest fluctuations in central collisions. Comparison with hydrodynamic models shows that the AMPT+iEBE-VISHNU with $\eta/s = 0.08$ and T$_R$ENTo +iEBE-VISHNU produce slightly larger flow angle fluctuations compared to the AMPT+iEBE-VISHNU with $\eta/s = 0.20$ in the 0%–5% central collisions. Still, neither of these models can describe the large flow angle fluctuations

observed in the data in this centrality interval. For the flow magnitude fluctuations, the hydrodynamic model calculations fail to describe the high-p_T deviation from unity in the 0%–5% central collisions. However, the AMPT+iEBE-VISHNU calculation with $\eta/s = 0.08$ is closest in describing the data. For noncentral collisions, the data are well described by the hydrodynamic calculations.

The flow angle fluctuations dominate all the measured centralities, although significant flow magnitude fluctuations are present, especially in central collisions. The measurements of the flow angle and flow magnitude fluctuations offer an improved understanding of the flow vector fluctuations. They can be used to constrain the initial conditions and transport coefficients of the QGP. Additionally, these measurements suggest that fluctuations of the flow angle are a feature of the system created in heavy-ion collisions and should be incorporated into nonhydrodynamical theoretical models used for comparison with high-p_T flow measurements, where such fluctuations are expected to be more pronounced.

ACKNOWLEDGMENTS

[1] E. V. Shuryak, Quark-gluon plasma and hadronic production of leptons, photons and psions, Phys. Lett. B **78**, 150 (1978).

[2] E. V. Shuryak, Quantum chromodynamics and the theory of superdense matter, Phys. Rep. **61**, 71 (1980).

[3] ALICE Collaboration, The ALICE experiment – A journey through QCD, arXiv:2211.04384.

[4] K. Adcox *et al.* (PHENIX Collaboration), Formation of dense partonic matter in relativistic nucleus-nucleus collisions at RHIC: Experimental evaluation by the PHENIX Collaboration, Nucl. Phys. A **757**, 184 (2005).

[5] I. Arsene *et al.* (BRAHMS Collaboration), Quark gluon plasma and color glass condensate at RHIC? The Perspective from the BRAHMS experiment, Nucl. Phys. A **757**, 1 (2005).

[6] B. B. Back *et al.*, The PHOBOS perspective on discoveries at RHIC, Nucl. Phys. A **757**, 28 (2005).

[7] J. Adams, Jr. *et al.* (STAR Collaboration), Experimental and theoretical challenges in the search for the quark gluon plasma: The STAR Collaboration's critical assessment of the evidence from RHIC collisions, Nucl. Phys. A **757**, 102 (2005).

[8] C. Gale, S. Jeon, and B. Schenke, Hydrodynamic modeling of heavy-ion collisions, Int. J. Mod. Phys. A **28**, 1340011 (2013).

[9] U. Heinz and R. Snellings, Collective flow and viscosity in relativistic heavy-ion collisions, Annu. Rev. Nucl. Part. Sci. **63**, 123 (2013).

[10] J.-Y. Ollitrault, Anisotropy as a signature of transverse collective flow, Phys. Rev. D **46**, 229 (1992).

[11] S. S. Adler *et al.* (PHENIX Collaboration), Elliptic flow of identified hadrons in Au+Au collisions at $\sqrt{s_{NN}} = 200$ GeV, Phys. Rev. Lett. **91**, 182301 (2003).

[12] J. Adams *et al.* (STAR Collaboration), Particle type dependence of azimuthal anisotropy and nuclear modification of particle production in Au + Au collisions at $\sqrt{s_{NN}} = 200$ GeV, Phys. Rev. Lett. **92**, 052302 (2004).

[13] J. Adams *et al.* (STAR Collaboration), Azimuthal anisotropy at the relativistic heavy ion collider: The first and fourth

harmonics, Phys. Rev. Lett. **92**, 062301 (2004); **127**, 069901(E) (2021).

[14] K. Aamodt *et al.* (ALICE Collaboration), Elliptic flow of charged particles in Pb–Pb collisions at 2.76 TeV, Phys. Rev. Lett. **105**, 252302 (2010).

[15] G. Aad *et al.* (ATLAS Collaboration), Measurement of the pseudorapidity and transverse momentum dependence of the elliptic flow of charged particles in lead-lead collisions at $\sqrt{s_{NN}} = 2.76$ TeV with the ATLAS detector, Phys. Lett. B **707**, 330 (2012).

[16] S. Chatrchyan *et al.* (CMS Collaboration), Measurement of the elliptic anisotropy of charged particles produced in PbPb collisions at $\sqrt{s_{NN}} = 2.76$ TeV, Phys. Rev. C **87**, 014902 (2013).

[17] S. Voloshin and Y. Zhang, Flow study in relativistic nuclear collisions by Fourier expansion of azimuthal particle distributions, Z. Phys. C **70**, 665 (1996).

[18] H. Niemi, G. S. Denicol, H. Holopainen, and P. Huovinen, Event-by-event distributions of azimuthal asymmetries in ultrarelativistic heavy-ion collisions, Phys. Rev. C **87**, 054901 (2013).

[19] B. Alver and G. Roland, Collision geometry fluctuations and triangular flow in heavy-ion collisions, Phys. Rev. C **81**, 054905 (2010); **82**, 039903(E) (2010).

[20] S. A. Voloshin, A. M. Poskanzer, A. Tang, and G. Wang, Elliptic flow in the Gaussian model of eccentricity fluctuations, Phys. Lett. B **659**, 537 (2008).

[21] B. Alver *et al.* (PHOBOS Collaboration), System size, energy, pseudorapidity, and centrality dependence of elliptic flow, Phys. Rev. Lett. **98**, 242302 (2007).

[22] B. H. Alver, C. Gombeaud, M. Luzum, and J.-Y. Ollitrault, Triangular flow in hydrodynamics and transport theory, Phys. Rev. C **82**, 034913 (2010).

[23] D. Teaney and L. Yan, Triangularity and Dipole Asymmetry in Heavy Ion Collisions, Phys. Rev. C **83**, 064904 (2011).

[24] M. Luzum, Collective flow and long-range correlations in relativistic heavy ion collisions, Phys. Lett. B **696**, 499 (2011).

[25] K. Aamodt *et al.* (ALICE Collaboration), Higher harmonic anisotropic flow measurements of charged particles in Pb–Pb collisions at $\sqrt{s_{NN}} = 2.76$ TeV, Phys. Rev. Lett. **107**, 032301 (2011).

[26] B. Abelev III *et al.* (ALICE Collaboration), Elliptic flow of identified hadrons in Pb–Pb collisions at $\sqrt{s_{NN}} = 2.76$ TeV, J. High Energy Phys. 06 (2015) 190.

[27] J. Adam *et al.* (ALICE Collaboration), Anisotropic flow of charged particles in Pb–Pb collisions at $\sqrt{s_{NN}} = 5.02$ TeV, Phys. Rev. Lett. **116**, 132302 (2016).

[28] S. Acharya *et al.* (ALICE Collaboration), Linear and non-linear flow modes in Pb–Pb collisions at $\sqrt{s_{NN}} = 2.76$ TeV, Phys. Lett. B **773**, 68 (2017).

[29] G. Aad *et al.* (ATLAS Collaboration), Measurement of the azimuthal anisotropy for charged particle production in $\sqrt{s_{NN}} = 2.76$ TeV lead-lead collisions with the ATLAS detector, Phys. Rev. C **86**, 014907 (2012).

[30] G. Aad *et al.* (ATLAS Collaboration), Measurement of the distributions of event-by-event flow harmonics in lead-lead collisions at $\sqrt{s_{NN}} = 2.76$ TeV with the ATLAS detector at the LHC, J. High Energy Phys. 11 (2013) 183.

[31] S. Chatrchyan Jr. *et al.* (CMS Collaboration), Centrality dependence of dihadron correlations and azimuthal anisotropy harmonics in PbPb collisions at $\sqrt{s_{NN}} = 2.76$ TeV, Eur. Phys. J. C **72**, 2012 (2012).

[32] S. Chatrchyan *et al.* (CMS Collaboration), Azimuthal anisotropy of charged particles at high transverse momenta in PbPb collisions at $\sqrt{s_{NN}} = 2.76$ TeV, Phys. Rev. Lett. **109**, 022301 (2012).

[33] M. Luzum and J.-Y. Ollitrault, Extracting the shear viscosity of the quark-gluon plasma from flow in ultra-central heavy-ion collisions, Nucl. Phys. A **904-905**, 377c (2013).

[34] C. Gale, S. Jeon, B. Schenke, P. Tribedy, and R. Venugopalan, Event-by-event anisotropic flow in heavy-ion collisions from combined Yang-Mills and viscous fluid dynamics, Phys. Rev. Lett. **110**, 012302 (2013).

[35] Z. Qiu and U. Heinz, Hydrodynamic event-plane correlations in Pb+Pb collisions at $\sqrt{s} = 2.76$ ATeV, Phys. Lett. B **717**, 261 (2012).

[36] D. Teaney and L. Yan, Event-plane correlations and hydrodynamic simulations of heavy ion collisions, Phys. Rev. C **90**, 024902 (2014).

[37] J. E. Bernhard, J. S. Moreland, and S. A. Bass, Bayesian estimation of the specific shear and bulk viscosity of quark–gluon plasma, Nat. Phys. **15**, 1113 (2019).

[38] D. Everett *et al.* (JETSCAPE Collaboration), Multisystem Bayesian constraints on the transport coefficients of QCD matter, Phys. Rev. C **103**, 054904 (2021).

[39] G. Nijs, W. van der Schee, U. Gürsoy, and R. Snellings, Bayesian analysis of heavy ion collisions with the heavy ion computational framework Trajectum, Phys. Rev. C **103**, 054909 (2021).

[40] V. Khachatryan, Jr. *et al.* (CMS Collaboration), Observation of long-range near-side angular correlations in proton-proton collisions at the LHC, J. High Energy Phys. 09 (2010) 091.

[41] K. Aamodt *et al.* (ALICE Collaboration), Harmonic decomposition of two-particle angular correlations in Pb–Pb collisions at $\sqrt{s_{NN}} = 2.76$ TeV, Phys. Lett. B **708**, 249 (2012).

[42] S. Chatrchyan, Jr. *et al.* (CMS Collaboration), Long-range and short-range dihadron angular correlations in central PbPb collisions at a nucleon-nucleon center of mass energy of 2.76 TeV, J. High Energy Phys. 07 (2011) 076.

[43] B. Abelev *et al.* (ALICE Collaboration), Long-range angular correlations on the near and away side in p-Pb collisions at $\sqrt{s_{NN}} = 5.02$ TeV, Phys. Lett. B **719**, 29 (2013).

[44] U. Heinz, Z. Qiu, and C. Shen, Fluctuating flow angles and anisotropic flow measurements, Phys. Rev. C **87**, 034913 (2013).

[45] F. G. Gardim, F. Grassi, M. Luzum, and J.-Y. Ollitrault, Breaking of factorization of two-particle correlations in hydrodynamics, Phys. Rev. C **87**, 031901(R) (2013).

[46] S. Acharya *et al.* (ALICE Collaboration), Searches for transverse momentum dependent flow vector fluctuations in Pb–Pb and p-Pb collisions at the LHC, J. High Energy Phys. 09 (2017) 032.

[47] V. Khachatryan *et al.* (CMS Collaboration), Evidence for transverse momentum and pseudorapidity dependent event plane fluctuations in PbPb and *p*Pb collisions, Phys. Rev. C **92**, 034911 (2015).

[48] R. S. Bhalerao, J.-Y. Ollitrault, S. Pal, and D. Teaney, Principal component analysis of event-by-event fluctuations, Phys. Rev. Lett. **114**, 152301 (2015).

[49] A. Mazeliauskas and D. Teaney, Subleading harmonic flows in hydrodynamic simulations of heavy ion collisions, Phys. Rev. C **91**, 044902 (2015).

[50] A. Mazeliauskas and D. Teaney, Fluctuations of harmonic and radial flow in heavy ion collisions

with principal components, Phys. Rev. C **93**, 024913 (2016).

[51] J. Milosevic, P. Cirkovic, D. Devetak, M. Dordevic, and M. Stojanovic, Sub-leading flow modes in PbPb collisions at $\sqrt{s_{NN}} = 2.76$ TeV from HYDJET++ model, EPJ Web Conf. **182**, 02086 (2018).

[52] P. Bożek, Principal component analysis of the nonlinear coupling of harmonic modes in heavy-ion collisions, Phys. Rev. C **97**, 034905 (2018).

[53] A. M. Sirunyan *et al.* (CMS Collaboration), Principal-component analysis of two-particle azimuthal correlations in PbPb and *p*Pb collisions at CMS, Phys. Rev. C **96**, 064902 (2017).

[54] M. Hippert, D. Dobrigkeit Chinellato, M. Luzum, J. Noronha, T. Nunes da Silva, and J. Takahashi, Measuring momentum-dependent flow fluctuations in heavy-ion collisions, Phys. Rev. C **101**, 034903 (2020).

[55] S. Acharya *et al.* (ALICE Collaboration), Pseudorapidity dependence of anisotropic flow and its decorrelations using long-range multiparticle correlations in Pb–Pb and Xe–Xe collisions, Phys. Lett. B **850**, 138477 (2024).

[56] S. Acharya *et al.* (ALICE Collaboration), Observation of flow angle and flow magnitude fluctuations in Pb–Pb collisions at $\sqrt{s_{NN}} = 5.02$ TeV at the CERN Large Hadron Collider, Phys. Rev. C **107**, L051901 (2023).

[57] A. Bilandzic, C. H. Christensen, K. Gulbrandsen, A. Hansen, and Y. Zhou, Generic framework for anisotropic flow analyses with multiparticle azimuthal correlations, Phys. Rev. C **89**, 064904 (2014).

[58] N. Borghini, P. M. Dinh, and J.-Y. Ollitrault, Flow analysis from multiparticle azimuthal correlations, Phys. Rev. C **64**, 054901 (2001).

[59] B. Alver *et al.* (PHOBOS Collaboration), Non-flow correlations and elliptic flow fluctuations in gold-gold collisions at $\sqrt{s_{NN}} = 200$ GeV, Phys. Rev. C **81**, 034915 (2010).

[60] D. Kikoła, L. Yi, S. Esumi, F. Wang, and W. Xie, Nonflow 'factorization' and a novel method to disentangle anisotropic flow and nonflow, Phys. Rev. C **86**, 014901 (2012).

[61] P. Bożek and W. Broniowski, Longitudinal decorrelation measures of flow magnitude and event-plane angles in ultrarelativistic nuclear collisions, Phys. Rev. C **97**, 034913 (2018).

[62] K. Aamodt *et al.* (ALICE Collaboration), The ALICE experiment at the CERN LHC, JINST **3**, S08002 (2008).

[63] K. Aamodt *et al.* (ALICE Collaboration), Alignment of the ALICE inner tracking system with cosmic-ray tracks, JINST **5**, P03003 (2010).

[64] J. Alme *et al.*, The ALICE TPC, a large 3-dimensional tracking device with fast readout for ultra-high multiplicity events, Nucl. Instrum. Methods Phys. Res., Sect. A **622**, 316 (2010).

[65] E. Abbas *et al.* (ALICE Collaboration), Performance of the ALICE VZERO system, J. Inst. **8**, P10016 (2013).

[66] B. Abelev *et al.* (ALICE Collaboration), Centrality determination of Pb–Pb collisions at $\sqrt{s_{NN}} = 2.76$ TeV with ALICE, Phys. Rev. C **88**, 044909 (2013).

[67] B. B. Abelev *et al.* (ALICE Collaboration), Performance of the ALICE Experiment at the CERN LHC, Int. J. Mod. Phys. A **29**, 1430044 (2014).

[68] B. Efron, Bootstrap methods: Another look at the jackknife, Ann. Stat. **7**, 1 (1979).

[69] X.-N. Wang and M. Gyulassy, HIJING: A Monte Carlo model for multiple jet production in pp, pA and AA collisions, Phys. Rev. D **44**, 3501 (1991).

[70] R. Barlow, Systematic errors: Facts and fictions, in *Conference on Advanced Statistical Techniques in Particle Physics* (Durham University Press, UK, 2002), pp. 134–144.

[71] W. Zhao, H.-J. Xu, and H. Song, Collective flow in 2.76 A TeV and 5.02 A TeV Pb+Pb collisions, Eur. Phys. J. C **77**, 645 (2017).

[72] C. Shen, Z. Qiu, H. Song, J. Bernhard, S. Bass, and U. Heinz, The iEBE-VISHNU code package for relativistic heavy-ion collisions, Comput. Phys. Commun. **199**, 61 (2016).

[73] J. S. Moreland, J. E. Bernhard, and S. A. Bass, Alternative ansatz to wounded nucleon and binary collision scaling in high-energy nuclear collisions, Phys. Rev. C **92**, 011901(R) (2015).

[74] Z.-W. Lin, C. M. Ko, B.-A. Li, B. Zhang, and S. Pal, A Multiphase transport model for relativistic heavy ion collisions, Phys. Rev. C **72**, 064901 (2005).

[75] E. G. Nielsen and Y. Zhou, Transverse momentum decorrelation of the flow vector in Pb–Pb collisions at $\sqrt{s_{NN}} = 5.02$ TeV, Eur. Phys. J. C **83**, 545 (2023).

S. Acharya ,[127] D. Adamová ,[86] A. Agarwal,[135] G. Aglieri Rinella ,[32] L. Aglietta,[24] M. Agnello ,[29] N. Agrawal ,[25] Z. Ahammed ,[135] S. Ahmad ,[15] S. U. Ahn ,[71] I. Ahuja ,[37] A. Akindinov ,[141] V. Akishina,[38] M. Al-Turany ,[97] D. Aleksandrov ,[141] B. Alessandro ,[56] H. M. Alfanda ,[6] R. Alfaro Molina ,[67] B. Ali ,[15] A. Alici ,[25] N. Alizadehvandchali ,[116] A. Alkin ,[104] J. Alme ,[20] G. Alocco ,[52] T. Alt ,[64] A. R. Altamura ,[50] I. Altsybeev ,[95] J. R. Alvarado ,[44] M. N. Anaam ,[6] C. Andrei ,[45] N. Andreou ,[115] A. Andronic ,[126] E. Andronov ,[141] V. Anguelov ,[94] F. Antinori ,[54] P. Antonioli ,[51] N. Apadula ,[74] L. Aphecetche ,[103] H. Appelshäuser ,[64] C. Arata ,[73] S. Arcelli ,[25] M. Aresti ,[22] R. Arnaldi ,[56] J. G. M. C. A. Arneiro ,[110] I. C. Arsene ,[19] M. Arslandok ,[138] A. Augustinus ,[32] R. Averbeck ,[97] M. D. Azmi ,[15] H. Baba,[124] A. Badalà ,[53] J. Bae ,[104] Y. W. Baek ,[40] X. Bai ,[120] R. Bailhache ,[64] Y. Bailung ,[48] R. Bala ,[91] A. Balbino ,[29] A. Baldisseri ,[130] B. Balis ,[2] D. Banerjee ,[4] Z. Banoo ,[91] V. Barbasova,[37] F. Barile ,[31] L. Barioglio ,[56] M. Barlou,[78] B. Barman,[41] G. G. Barnaföldi ,[46] L. S. Barnby ,[115] E. Barreau ,[103] V. Barret ,[127] L. Barreto ,[110] C. Bartels ,[119] K. Barth ,[32] E. Bartsch ,[64] N. Bastid ,[127] S. Basu ,[75] G. Batigne ,[103] D. Battistini ,[95] B. Batyunya ,[142] D. Bauri,[47] J. L. Bazo Alba ,[101] I. G. Bearden ,[83] C. Beattie ,[138] P. Becht ,[97] D. Behera ,[48] I. Belikov ,[129] A. D. C. Bell Hechavarria ,[126] F. Bellini ,[25] R. Bellwied ,[116] S. Belokurova ,[141] L. G. E. Beltran ,[109] Y. A. V. Beltran ,[44] G. Bencedi ,[46] A. Bensaoula,[116] S. Beole ,[24] Y. Berdnikov ,[141] A. Berdnikova ,[94] L. Bergmann ,[94] M. G. Besoiu ,[63] L. Betev ,[32] P. P. Bhaduri ,[135] A. Bhasin ,[91] M. A. Bhat ,[4]

B. Bhattacharjee [41] L. Bianchi [24] N. Bianchi [49] J. Bielčík [35] J. Bielčíková [86] A. P. Bigot [129] A. Bilandzic [95]
G. Biro [46] S. Biswas [4] N. Bize [103] J. T. Blair [108] D. Blau [141] M. B. Blidaru [97] N. Bluhme [38] C. Blume [64]
G. Boca [21,55] F. Bock [87] T. Bodova [20] J. Bok [16] L. Boldizsár [46] M. Bombara [37] P. M. Bond [32] G. Bonomi [134,55]
H. Borel [130] A. Borissov [141] A. G. Borquez Carcamo [94] H. Bossi [138] E. Botta [24] Y. E. M. Bouziani [64]
L. Bratrud [64] P. Braun-Munzinger [97] M. Bregant [110] M. Broz [35] G. E. Bruno [96,31] M. D. Buckland [23]
D. Budnikov [141] H. Buesching [64] S. Bufalino [29] P. Buhler [102] N. Burmasov [141] Z. Buthelezi [68,123] A. Bylinkin [20]
S. A. Bysiak [107] J. C. Cabanillas Noris [109] M. F. T. Cabrera [116] M. Cai [6] H. Caines [138] A. Caliva [28] E. Calvo Villar [101]
J. M. M. Camacho [109] P. Camerini [23] F. D. M. Canedo [110] S. L. Cantway [138] M. Carabas [113] A. A. Carballo [32]
F. Carnesecchi [32] R. Caron [128] L. A. D. Carvalho [110] J. Castillo Castellanos [130] M. Castoldi [32] F. Catalano [32]
S. Cattaruzzi [23] C. Ceballos Sanchez [142] R. Cerri [24] I. Chakaberia [74] P. Chakraborty [136,47] S. Chandra [135]
S. Chapeland [32] M. Chartier [119] S. Chattopadhyay [135] S. Chattopadhyay [135] S. Chattopadhyay [99] T. Cheng [97,6]
C. Cheshkov [128] V. Chibante Barroso [32] D. D. Chinellato [111] E. S. Chizzali [95,a] J. Cho [58] S. Cho [58] P. Chochula [32]
Z. A. Chochulska [136] D. Choudhury [41] P. Christakoglou [84] C. H. Christensen [83] P. Christiansen [75] T. Chujo [125]
M. Ciacco [29] C. Cicalo [52] M. R. Ciupek [97] G. Clai [51,b] F. Colamaria [50] J. S. Colburn [100] D. Colella [96,31] M. Colocci [25]
M. Concas [32] G. Conesa Balbastre [73] Z. Conesa del Valle [131] G. Contin [23] J. G. Contreras [35] M. L. Coquet [103,130]
P. Cortese [133,56] M. R. Cosentino [112] F. Costa [32] S. Costanza [21,55] C. Cot [131] J. Crkovská [94] P. Crochet [127]
R. Cruz-Torres [74] P. Cui [6] A. Dainese [54] G. Dange [38] M. C. Danisch [94] A. Danu [63] P. Das [80] P. Das [4] S. Das [4]
A. R. Dash [126] S. Dash [47] A. De Caro [28] G. de Cataldo [50] J. de Cuveland [38] A. De Falco [22] D. De Gruttola [28]
N. De Marco [56] C. De Martin [23] S. De Pasquale [28] R. Deb [134] R. Del Grande [95] L. Dello Stritto [32] W. Deng [6]
K. C. Devereaux [18] P. Dhankher [18] D. Di Bari [31] A. Di Mauro [32] B. Diab [130] R. A. Diaz [142,7] T. Dietel [114]
Y. Ding [6] J. Ditzel [64] R. Divià [32] D. U. Dixit [18] Ø. Djuvsland [20] U. Dmitrieva [141] A. Dobrin [63] B. Dönigus [64]
J. M. Dubinski [136] A. Dubla [97] S. Dudi [90] P. Dupieux [127] N. Dzalaiova [13] T. M. Eder [126] R. J. Ehlers [74]
F. Eisenhut [64] R. Ejima [92] D. Elia [50] B. Erazmus [103] F. Ercolessi [25] B. Espagnon [131] G. Eulisse [32] D. Evans [100]
S. Evdokimov [141] L. Fabbietti [95] M. Faggin [27] J. Faivre [73] F. Fan [6] W. Fan [74] A. Fantoni [49] M. Fasel [87]
A. Feliciello [56] G. Feofilov [141] A. Fernández Téllez [44] L. Ferrandi [110] M. B. Ferrer [32] A. Ferrero [130]
C. Ferrero [56,c] A. Ferretti [24] V. J. G. Feuillard [94] V. Filova [35] D. Finogeev [141] F. M. Fionda [52] E. Flatland [32]
F. Flor [116] A. N. Flores [108] S. Foertsch [68] I. Fokin [94] S. Fokin [141] U. Follo [56,c] E. Fragiacomo [57] E. Frajna [46]
U. Fuchs [32] N. Funicello [28] C. Furget [73] A. Furs [141] T. Fusayasu [98] J. J. Gaardhøje [83] M. Gagliardi [24]
A. M. Gago [101] T. Gahlaut [47] C. D. Galvan [109] D. R. Gangadharan [116] P. Ganoti [78] C. Garabatos [97] J. M. Garcia [44]
T. García Chávez [44] E. Garcia-Solis [9] C. Gargiulo [32] P. Gasik [97] H. M. Gaur [38] A. Gautam [118] M. B. Gay Ducati [66]
M. Germain [103] A. Ghimouz [125] C. Ghosh [135] M. Giacalone [51] G. Gioachin [29] P. Giubellino [97,56] P. Giubilato [27]
A. M. C. Glaenzer [130] P. Glässel [94] E. Glimos [122] D. J. Q. Goh [76] V. Gonzalez [137] P. Gordeev [141] M. Gorgon [2]
K. Goswami [48] S. Gotovac [33] V. Grabski [67] L. K. Graczykowski [136] E. Grecka [86] A. Grelli [59] C. Grigoras [32]
V. Grigoriev [141] S. Grigoryan [142,1] F. Grosa [32] J. F. Grosse-Oetringhaus [32] R. Grosso [97] D. Grund [35]
N. A. Grunwald [94] G. G. Guardiano [111] R. Guernane [73] M. Guilbaud [103] K. Gulbrandsen [83] T. Gündem [64]
T. Gunji [124] W. Guo [6] A. Gupta [91] R. Gupta [91] R. Gupta [48] K. Gwizdziel [136] L. Gyulai [46] C. Hadjidakis [131]
F. U. Haider [91] S. Haidlova [35] M. Haldar [4] H. Hamagaki [76] A. Hamdi [74] Y. Han [139] B. G. Hanley [137]
R. Hannigan [108] J. Hansen [75] M. R. Haque [97] J. W. Harris [138] A. Harton [9] M. V. Hartung [64] H. Hassan [117]
D. Hatzifotiadou [51] P. Hauer [42] L. B. Havener [138] E. Hellbär [97] H. Helstrup [34] M. Hemmer [64] T. Herman [35]
S. G. Hernandez [116] G. Herrera Corral [8] F. Herrmann [126] S. Herrmann [128] K. F. Hetland [34] B. Heybeck [64]
H. Hillemanns [32] B. Hippolyte [129] F. W. Hoffmann [70] B. Hofman [59] G. H. Hong [139] M. Horst [95] A. Horzyk [2]
Y. Hou [6] P. Hristov [32] P. Huhn [64] L. M. Huhta [117] T. J. Humanic [88] A. Hutson [116] D. Hutter [38] M. C. Hwang [18]
R. Ilkaev [141] M. Inaba [125] G. M. Innocenti [32] M. Ippolitov [141] A. Isakov [84] T. Isidori [118] M. S. Islam [99]
S. Iurchenko [141] M. Ivanov [13] M. Ivanov [97] V. Ivanov [141] K. E. Iversen [75] M. Jablonski [2] B. Jacak [18,74] N. Jacazio [25]
P. M. Jacobs [74] S. Jadlovska [106] J. Jadlovsky [106] S. Jaelani [82] C. Jahnke [110] M. J. Jakubowska [136] M. A. Janik [136]
T. Janson [70] S. Ji [16] S. Jia [10] A. A. P. Jimenez [65] F. Jonas [74] D. M. Jones [119] J. M. Jowett [32,97] J. Jung [64]
M. Jung [64] A. Junique [32] A. Jusko [100] J. Kaewjai [105] P. Kalinak [60] A. Kalweit [32] A. Karasu Uysal [72,d]
D. Karatovic [89] O. Karavichev [141] T. Karavicheva [141] E. Karpechev [141] M. J. Karwowska [32,136] U. Kebschull [70]
R. Keidel [140] M. Keil [32] B. Ketzer [42] S. S. Khade [48] A. M. Khan [120] S. Khan [15] A. Khanzadeev [141]
Y. Kharlov [141] A. Khatun [118] A. Khuntia [35] Z. Khuranova [64] B. Kileng [34] B. Kim [104] C. Kim [16] D. J. Kim [117]
E. J. Kim [69] J. Kim [139] J. Kim [58] J. Kim [69] M. Kim [18] S. Kim [17] T. Kim [139] K. Kimura [92] A. Kirkova [36]
S. Kirsch [64] I. Kisel [38] S. Kiselev [141] A. Kisiel [136] J. P. Kitowski [2] J. L. Klay [5] J. Klein [32] S. Klein [74]
C. Klein-Bösing [126] M. Kleiner [64] T. Klemenz [95] A. Kluge [32] C. Kobdaj [105] R. Kohara [124] T. Kollegger [97]
A. Kondratyev [142] N. Kondratyeva [141] J. Konig [64] S. A. Konigstorfer [95] P. J. Konopka [32] G. Kornakov [136]
M. Korwieser [95] S. D. Koryciak [2] C. Koster [84] A. Kotliarov [86] N. Kovacic [89] V. Kovalenko [141] M. Kowalski [107]
V. Kozhuharov [36] I. Králik [60] A. Kravčáková [37] L. Krcal [32,38] M. Krivda [100,60] F. Krizek [86]
K. Krizkova Gajdosova [32] C. Krug [66] M. Krüger [64] D. M. Krupova [35] E. Kryshen [141] V. Kučera [58] C. Kuhn [129]
P. G. Kuijer [84] T. Kumaoka [125] D. Kumar [135] L. Kumar [90] N. Kumar [90] S. Kumar [31] S. Kundu [32] P. Kurashvili [79]

A. Kurepin [141] A. B. Kurepin [141] A. Kuryakin [141] S. Kushpil [86] V. Kuskov [141] M. Kutyla,[136] M. J. Kweon [58]
Y. Kwon [139] S. L. La Pointe [38] P. La Rocca [26] A. Lakrathok,[105] M. Lamanna [32] A. R. Landou [73] R. Langoy [121]
P. Larionov [32] E. Laudi [32] L. Lautner [32,95] R. A. N. Laveaga,[109] R. Lavicka [102] R. Lea [134,55] H. Lee [104]
I. Legrand [45] G. Legras [126] J. Lehrbach [38] T. M. Lelek,[2] R. C. Lemmon [85] I. León Monzón [109] M. M. Lesch [95]
E. D. Lesser [18] P. Lévai [46] M. Li,[6] X. Li,[10] B. E. Liang-gilman [18] J. Lien [121] R. Lietava [100] I. Likmeta [116]
B. Lim [24] S. H. Lim [16] V. Lindenstruth [38] A. Lindner,[45] C. Lippmann [97] D. H. Liu,[6] J. Liu [119]
G. S. S. Liveraro [111] I. M. Lofnes [20] C. Loizides [87] S. Lokos [107] J. Lömker [59] X. Lopez [127] E. López Torres [7]
P. Lu [97,120] F. V. Lugo [67] J. R. Luhder [126] M. Lunardon [27] G. Luparello [57] Y. G. Ma [39] M. Mager [32] A. Maire [129]
E. M. Majerz,[2] M. V. Makariev [36] M. Malaev [141] G. Malfattore [25] N. M. Malik [91] Q. W. Malik,[19] S. K. Malik [91]
L. Malinina [142,e,f] D. Mallick [131] N. Mallick [48] G. Mandaglio [30,53] S. K. Mandal [79] A. Manea [63] V. Manko [141]
F. Manso [127] V. Manzari [50] Y. Mao [6] R. W. Marcjan [2] G. V. Margagliotti [23] A. Margotti [51] A. Marín [97]
C. Markert [108] P. Martinengo [32] M. I. Martínez [44] G. Martínez García [103] M. P. P. Martins [110] S. Masciocchi [97]
M. Masera [24] A. Masoni [52] L. Massacrier [131] O. Massen [59] A. Mastroserio [132,50] O. Matonoha [75] S. Mattiazzo [27]
A. Matyja [107] A. L. Mazuecos [32] F. Mazzaschi [24] M. Mazzilli [116] J. E. Mdhluli [123] Y. Melikyan [43]
A. Menchaca-Rocha [67] J. E. M. Mendez [65] E. Meninno [102] A. S. Menon [116] M. W. Menzel,[32,94] M. Meres [13]
Y. Miake,[125] L. Micheletti [32] D. L. Mihaylov [95] K. Mikhaylov [142,141] N. Minafra [118] D. Miśkowiec [97] A. Modak [4]
B. Mohanty,[80] M. Mohisin Khan [15,g] M. A. Molander [43] S. Monira [136] C. Mordasini [117] D. A. Moreira De Godoy [126]
I. Morozov [141] A. Morsch [32] T. Mrnjavac [32] V. Muccifora [49] S. Muhuri [135] J. D. Mulligan [74] A. Mulliri [22]
M. G. Munhoz [110] R. H. Munzer [64] H. Murakami [124] S. Murray [114] L. Musa [32] J. Musinsky [60] J. W. Myrcha [136]
B. Naik [123] A. I. Nambrath [18] B. K. Nandi [47] R. Nania [51] E. Nappi [50] A. F. Nassirpour [17] A. Nath [94]
C. Nattrass [122] M. N. Naydenov [36] A. Neagu,[19] A. Negru,[113] E. Nekrasova,[141] L. Nellen [65] R. Nepeivoda [75]
S. Nese [19] G. Neskovic [38] N. Nicassio [50] B. S. Nielsen [83] E. G. Nielsen [83] S. Nikolaev [141] S. Nikulin [141]
V. Nikulin [141] F. Noferini [51] S. Noh [12] P. Nomokonov [142] J. Norman [119] N. Novitzky [87] P. Nowakowski [136]
A. Nyanin [141] J. Nystrand [20] S. Oh [17] A. Ohlson [75] V. A. Okorokov [141] J. Oleniacz [136] A. Onnerstad [117]
C. Oppedisano [56] A. Ortiz Velasquez [65] J. Otwinowski [107] M. Oya,[92] K. Oyama [76] Y. Pachmayer [94] S. Padhan [47]
D. Pagano [134,55] G. Paić [65] S. Paisano-Guzmán [44] A. Palasciano [50] S. Panebianco [130] H. Park [125] H. Park [104]
J. E. Parkkila [32] Y. Patley [47] B. Paul [22] M. M. D. M. Paulino [110] H. Pei [6] T. Peitzmann [59] X. Peng [11]
M. Pennisi [24] S. Perciballi [24] D. Peresunko [141] G. M. Perez [7] Y. Pestov,[141] V. Petrov,[141] M. Petrovici [45]
S. Piano [57] M. Pikna [13] P. Pillot [103] O. Pinazza [51,32] L. Pinsky,[116] C. Pinto [95] S. Pisano [49] M. Płoskoń [74]
M. Planinic,[89] F. Pliquett,[64] M. G. Poghosyan [87] B. Polichtchouk [141] S. Politano [29] N. Poljak [89] A. Pop [45]
S. Porteboeuf-Houssais [127] V. Pozdniakov [142,e] I. Y. Pozos [44] K. K. Pradhan [48] S. K. Prasad [4] S. Prasad [48]
R. Preghenella [51] F. Prino [56] C. A. Pruneau [137] I. Pshenichnov [141] M. Puccio [32] S. Pucillo [24] S. Qiu [84]
L. Quaglia [24] S. Ragoni [14] A. Rai [138] A. Rakotozafindrabe [130] L. Ramello [133,56] F. Rami [129] M. Rasa [26]
S. S. Räsänen [43] R. Rath [51] M. P. Rauch [20] I. Ravasenga [32] K. F. Read [87,122] C. Reckziegel [112] A. R. Redelbach [38]
K. Redlich [79,h] C. A. Reetz [97] H. D. Regules-Medel,[44] A. Rehman,[20] F. Reidt [32] H. R. Reme-Ness [34] Z. Rescakova,[37]
K. Reygers [94] A. Riabov [141] V. Riabov [141] R. Ricci [28] M. Richter [20] A. A. Riedel [95] W. Riegler [32]
A. G. Riffero [24] C. Ripoli,[28] C. Ristea [63] M. V. Rodriguez [32] M. Rodríguez Cahuantzi [44] S. A. Rodríguez Ramírez [44]
K. Røed [19] R. Rogalev [141] E. Rogochaya [142] T. S. Rogoschinski [64] D. Rohr [32] D. Röhrich [20] S. Rojas Torres [35]
P. S. Rokita [136] G. Romanenko [25] F. Ronchetti [49] E. D. Rosas,[65] K. Roslon [136] A. Rossi [54] A. Roy [48] S. Roy [47]
N. Rubini [25] D. Ruggiano [136] R. Rui [23] P. G. Russek [2] R. Russo [84] A. Rustamov [81] E. Ryabinkin [141]
Y. Ryabov [141] A. Rybicki [107] J. Ryu [16] W. Rzesa [136] S. Sadhu [31] S. Sadovsky [141] J. Saetre [20] K. Šafařík [35]
S. K. Saha [4] S. Saha [80] B. Sahoo [48] R. Sahoo [48] S. Sahoo,[61] D. Sahu [48] P. K. Sahu [61] J. Saini [135] K. Sajdakova,[37]
S. Sakai [125] M. P. Salvan [97] S. Sambyal [91] D. Samitz [102] I. Sanna [32,95] T. B. Saramela [110] D. Sarkar [83] P. Sarma [41]
V. Sarritzu [22] V. M. Sarti [95] M. H. P. Sas [32] S. Sawan [80] E. Scapparone [51] J. Schambach [87] H. S. Scheid [64]
C. Schiaua [45] R. Schicker [94] F. Schlepper [94] A. Schmah,[97] C. Schmidt [97] H. R. Schmidt,[93] M. O. Schmidt [32]
M. Schmidt,[93] N. V. Schmidt [87] A. R. Schmier [122] R. Schotter [129] A. Schröter [38] J. Schukraft [32] K. Schweda [97]
G. Scioli [25] E. Scomparin [56] J. E. Seger [14] Y. Sekiguchi [124] D. Sekihata [124] M. Selina [84] I. Selyuzhenkov [97]
S. Senyukov [129] J. J. Seo [94] D. Serebryakov [141] L. Serkin [65] L. Šerkšnytė [95] A. Sevcenco [63] T. J. Shaba [68]
A. Shabetai [103] R. Shahoyan,[32] A. Shangaraev [141] B. Sharma [91] D. Sharma [47] H. Sharma [54] M. Sharma [91]
S. Sharma [76] S. Sharma [91] U. Sharma [91] A. Shatat [131] O. Sheibani,[116] K. Shigaki [92] M. Shimomura,[77] J. Shin,[12]
S. Shirinkin [141] Q. Shou [39] Y. Sibiriak [141] S. Siddhanta [52] T. Siemiarczuk [79] T. F. Silva [110] D. Silvermyr [75]
T. Simantathammakul,[105] R. Simeonov [36] B. Singh,[91] B. Singh [95] K. Singh [48] R. Singh [80] R. Singh [91] R. Singh [97,48]
S. Singh [15] V. K. Singh [135] V. Singhal [135] T. Sinha [99] B. Sitar [13] M. Sitta [133,56] T. B. Skaali,[19] G. Skorodumovs [94]
N. Smirnov [138] R. J. M. Snellings [59] E. H. Solheim [19] J. Song [16] C. Sonnabend [32,97] J. M. Sonneveld [84]
F. Soramel [27] A. B. Soto-hernandez [88] R. Spijkers [84] I. Sputowska [107] J. Staa [75] J. Stachel [94] I. Stan [63]
P. J. Steffanic [122] S. F. Stiefelmaier [94] D. Stocco [103] I. Storehaug [19] N. J. Strangmann [64] P. Stratmann [126]
S. Strazzi [25] A. Sturniolo [30,53] C. P. Stylianidis,[84] A. A. P. Suaide [110] C. Suire [131] M. Sukhanov [141] M. Suljic [32]
R. Sultanov [141] V. Sumberia [91] S. Sumowidagdo [82] I. Szarka [13] M. Szymkowski [136] S. F. Taghavi [95]

G. Taillepied [97] J. Takahashi [111] G. J. Tambave [80] S. Tang [6] Z. Tang [120] J. D. Tapia Takaki [118] N. Tapus,[113] L. A. Tarasovicova [126] M. G. Tarzila [45] G. F. Tassielli [31] A. Tauro [32] A. Tavira García [131] G. Tejeda Muñoz [44] A. Telesca [32] L. Terlizzi [24] C. Terrevoli [50] S. Thakur [4] D. Thomas [108] A. Tikhonov [141] N. Tiltmann [32,126] A. R. Timmins [116] M. Tkacik,[106] T. Tkacik [106] A. Toia [64] R. Tokumoto,[92] S. Tomassini,[25] K. Tomohiro,[92] N. Topilskaya [141] M. Toppi [49] T. Tork [131] V. V. Torres [103] A. G. Torres Ramos [31] A. Trifiró [30,53] A. S. Triolo [32,30,53] S. Tripathy [32] T. Tripathy [47] V. Trubnikov [3] W. H. Trzaska [117] T. P. Trzcinski [136] A. Tumkin,[141] R. Turrisi [54] T. S. Tveter [19] K. Ullaland [20] B. Ulukutlu [95] A. Uras [128] M. Urioni [134] G. L. Usai [22] M. Vala,[37] N. Valle [55] L. V. R. van Doremalen,[59] M. van Leeuwen [84] C. A. van Veen [94] R. J. G. van Weelden [84] P. Vande Vyvre [32] D. Varga [46] Z. Varga [46] P. Vargas Torres,[65] M. Vasileiou [78] A. Vasiliev [141] O. Vázquez Doce [49] O. Vazquez Rueda [116] V. Vechernin [141] E. Vercellin [24] S. Vergara Limón,[44] R. Verma,[47] L. Vermunt [97] R. Vértesi [46] M. Verweij [59] L. Vickovic,[33] Z. Vilakazi,[123] O. Villalobos Baillie [100] A. Villani [23] A. Vinogradov [141] T. Virgili [28] M. M. O. Virta [117] V. Vislavicius [75] A. Vodopyanov [142] B. Volkel [32] M. A. Völkl [94] S. A. Voloshin [137] G. Volpe [31] B. von Haller [32] I. Vorobyev [32] N. Vozniuk [141] J. Vrláková [37] J. Wan,[39] C. Wang [39] D. Wang,[39] Y. Wang [39] Y. Wang [6] A. Wegrzynek [32] F. T. Weiglhofer,[38] S. C. Wenzel [32] J. P. Wessels [126] J. Wiechula [64] J. Wikne [19] G. Wilk [79] J. Wilkinson [97] G. A. Willems [126] B. Windelband [94] M. Winn [130] J. R. Wright [108] W. Wu,[39] Y. Wu [120] Z. Xiong,[120] R. Xu [6] A. Yadav [42] A. K. Yadav [135] Y. Yamaguchi [92] S. Yang,[20] S. Yano [92] E. R. Yeats,[18] Z. Yin [6] I.-K. Yoo [16] J. H. Yoon [58] H. Yu,[12] S. Yuan,[20] A. Yuncu [94] V. Zaccolo [23] C. Zampolli [32] M. Zang,[6] F. Zanone [94] N. Zardoshti [32] A. Zarochentsev [141] P. Závada [62] N. Zaviyalov,[141] M. Zhalov [141] B. Zhang [6] C. Zhang [130] L. Zhang [39] M. Zhang,[6] S. Zhang [39] X. Zhang [6] Y. Zhang,[120] Z. Zhang [6] M. Zhao [10] V. Zherebchevskii [141] Y. Zhi,[10] C. Zhong,[39] D. Zhou [6] Y. Zhou [83] J. Zhu [54,6] S. Zhu,[120] Y. Zhu,[6] S. C. Zugravel [56] and N. Zurlo [134,55]

(ALICE Collaboration)

[1]*A.I. Alikhanyan National Science Laboratory (Yerevan Physics Institute) Foundation, Yerevan, Armenia*
[2]*AGH University of Krakow, Cracow, Poland*
[3]*Bogolyubov Institute for Theoretical Physics, National Academy of Sciences of Ukraine, Kiev, Ukraine*
[4]*Bose Institute, Department of Physics and Centre for Astroparticle Physics and Space Science (CAPSS), Kolkata, India*
[5]*California Polytechnic State University, San Luis Obispo, California, USA*
[6]*Central China Normal University, Wuhan, China*
[7]*Centro de Aplicaciones Tecnológicas y Desarrollo Nuclear (CEADEN), Havana, Cuba*
[8]*Centro de Investigación y de Estudios Avanzados (CINVESTAV), Mexico City and Mérida, Mexico*
[9]*Chicago State University, Chicago, Illinois, USA*
[10]*China Institute of Atomic Energy, Beijing, China*
[11]*China University of Geosciences, Wuhan, China*
[12]*Chungbuk National University, Cheongju, Republic of Korea*
[13]*Comenius University Bratislava, Faculty of Mathematics, Physics and Informatics, Bratislava, Slovak Republic*
[14]*Creighton University, Omaha, Nebraska, USA*
[15]*Department of Physics, Aligarh Muslim University, Aligarh, India*
[16]*Department of Physics, Pusan National University, Pusan, Republic of Korea*
[17]*Department of Physics, Sejong University, Seoul, Republic of Korea*
[18]*Department of Physics, University of California, Berkeley, California, USA*
[19]*Department of Physics, University of Oslo, Oslo, Norway*
[20]*Department of Physics and Technology, University of Bergen, Bergen, Norway*
[21]*Dipartimento di Fisica, Università di Pavia, Pavia, Italy*
[22]*Dipartimento di Fisica dell'Università and Sezione INFN, Cagliari, Italy*
[23]*Dipartimento di Fisica dell'Università and Sezione INFN, Trieste, Italy*
[24]*Dipartimento di Fisica dell'Università and Sezione INFN, Turin, Italy*
[25]*Dipartimento di Fisica e Astronomia dell'Università and Sezione INFN, Bologna, Italy*
[26]*Dipartimento di Fisica e Astronomia dell'Università and Sezione INFN, Catania, Italy*
[27]*Dipartimento di Fisica e Astronomia dell'Università and Sezione INFN, Padova, Italy*
[28]*Dipartimento di Fisica 'E.R. Caianiello' dell'Università and Gruppo Collegato INFN, Salerno, Italy*
[29]*Dipartimento DISAT del Politecnico and Sezione INFN, Turin, Italy*
[30]*Dipartimento di Scienze MIFT, Università di Messina, Messina, Italy*
[31]*Dipartimento Interateneo di Fisica 'M. Merlin' and Sezione INFN, Bari, Italy*
[32]*European Organization for Nuclear Research (CERN), Geneva, Switzerland*
[33]*Faculty of Electrical Engineering, Mechanical Engineering and Naval Architecture, University of Split, Split, Croatia*
[34]*Faculty of Engineering and Science, Western Norway University of Applied Sciences, Bergen, Norway*
[35]*Faculty of Nuclear Sciences and Physical Engineering, Czech Technical University in Prague, Prague, Czech Republic*

[36]*Faculty of Physics, Sofia University, Sofia, Bulgaria*

[37]*Faculty of Science, P.J. Šafárik University, Košice, Slovak Republic*

[38]*Frankfurt Institute for Advanced Studies, Johann Wolfgang Goethe-Universität Frankfurt, Frankfurt, Germany*

[39]*Fudan University, Shanghai, China*

[40]*Gangneung-Wonju National University, Gangneung, Republic of Korea*

[41]*Gauhati University, Department of Physics, Guwahati, India*

[42]*Helmholtz-Institut für Strahlen- und Kernphysik, Rheinische Friedrich-Wilhelms-Universität Bonn, Bonn, Germany*

[43]*Helsinki Institute of Physics (HIP), Helsinki, Finland*

[44]*High Energy Physics Group, Universidad Autónoma de Puebla, Puebla, Mexico*

[45]*Horia Hulubei National Institute of Physics and Nuclear Engineering, Bucharest, Romania*

[46]*HUN-REN Wigner Research Centre for Physics, Budapest, Hungary*

[47]*Indian Institute of Technology Bombay (IIT), Mumbai, India*

[48]*Indian Institute of Technology Indore, Indore, India*

[49]*INFN, Laboratori Nazionali di Frascati, Frascati, Italy*

[50]*INFN, Sezione di Bari, Bari, Italy*

[51]*INFN, Sezione di Bologna, Bologna, Italy*

[52]*INFN, Sezione di Cagliari, Cagliari, Italy*

[53]*INFN, Sezione di Catania, Catania, Italy*

[54]*INFN, Sezione di Padova, Padova, Italy*

[55]*INFN, Sezione di Pavia, Pavia, Italy*

[56]*INFN, Sezione di Torino, Turin, Italy*

[57]*INFN, Sezione di Trieste, Trieste, Italy*

[58]*Inha University, Incheon, Republic of Korea*

[59]*Institute for Gravitational and Subatomic Physics (GRASP), Utrecht University/Nikhef, Utrecht, Netherlands*

[60]*Institute of Experimental Physics, Slovak Academy of Sciences, Košice, Slovak Republic*

[61]*Institute of Physics, Homi Bhabha National Institute, Bhubaneswar, India*

[62]*Institute of Physics of the Czech Academy of Sciences, Prague, Czech Republic*

[63]*Institute of Space Science (ISS), Bucharest, Romania*

[64]*Institut für Kernphysik, Johann Wolfgang Goethe-Universität Frankfurt, Frankfurt, Germany*

[65]*Instituto de Ciencias Nucleares, Universidad Nacional Autónoma de México, Mexico City, Mexico*

[66]*Instituto de Física, Universidade Federal do Rio Grande do Sul (UFRGS), Porto Alegre, Brazil*

[67]*Instituto de Física, Universidad Nacional Autónoma de México, Mexico City, Mexico*

[68]*iThemba LABS, National Research Foundation, Somerset West, South Africa*

[69]*Jeonbuk National University, Jeonju, Republic of Korea*

[70]*Johann-Wolfgang-Goethe Universität Frankfurt Institut für Informatik, Fachbereich Informatik und Mathematik, Frankfurt, Germany*

[71]*Korea Institute of Science and Technology Information, Daejeon, Republic of Korea*

[72]*KTO Karatay University, Konya, Turkey*

[73]*Laboratoire de Physique Subatomique et de Cosmologie, Université Grenoble-Alpes, CNRS-IN2P3, Grenoble, France*

[74]*Lawrence Berkeley National Laboratory, Berkeley, California, USA*

[75]*Lund University Department of Physics, Division of Particle Physics, Lund, Sweden*

[76]*Nagasaki Institute of Applied Science, Nagasaki, Japan*

[77]*Nara Women's University (NWU), Nara, Japan*

[78]*National and Kapodistrian University of Athens, School of Science, Department of Physics, Athens, Greece*

[79]*National Centre for Nuclear Research, Warsaw, Poland*

[80]*National Institute of Science Education and Research, Homi Bhabha National Institute, Jatni, India*

[81]*National Nuclear Research Center, Baku, Azerbaijan*

[82]*National Research and Innovation Agency - BRIN, Jakarta, Indonesia*

[83]*Niels Bohr Institute, University of Copenhagen, Copenhagen, Denmark*

[84]*Nikhef, National Institute for Subatomic Physics, Amsterdam, Netherlands*

[85]*Nuclear Physics Group, STFC Daresbury Laboratory, Daresbury, United Kingdom*

[86]*Nuclear Physics Institute of the Czech Academy of Sciences, Husinec-Řež, Czech Republic*

[87]*Oak Ridge National Laboratory, Oak Ridge, Tennessee, USA*

[88]*Ohio State University, Columbus, Ohio, USA*

[89]*Physics Department, Faculty of Science, University of Zagreb, Zagreb, Croatia*

[90]*Physics Department, Panjab University, Chandigarh, India*

[91]*Physics Department, University of Jammu, Jammu, India*

[92]*Physics Program and International Institute for Sustainability with Knotted Chiral Meta Matter (SKCM2), Hiroshima University, Hiroshima, Japan*

[93]*Physikalisches Institut, Eberhard-Karls-Universität Tübingen, Tübingen, Germany*

[94]*Physikalisches Institut, Ruprecht-Karls-Universität Heidelberg, Heidelberg, Germany*

[95]*Physik Department, Technische Universität München, Munich, Germany*

[96]*Politecnico di Bari and Sezione INFN, Bari, Italy*

[97]*Research Division and ExtreMe Matter Institute EMMI, GSI Helmholtzzentrum für Schwerionenforschung GmbH, Darmstadt, Germany*

[98]*Saga University, Saga, Japan*

[99]*Saha Institute of Nuclear Physics, Homi Bhabha National Institute, Kolkata, India*

[100]*School of Physics and Astronomy, University of Birmingham, Birmingham, United Kingdom*

[101]*Sección Física, Departamento de Ciencias, Pontificia Universidad Católica del Perú, Lima, Peru*

[102]*Stefan Meyer Institut für Subatomare Physik (SMI), Vienna, Austria*

[103]*SUBATECH, IMT Atlantique, Nantes Université, CNRS-IN2P3, Nantes, France*

[104]*Sungkyunkwan University, Suwon City, Republic of Korea*

[105]*Suranaree University of Technology, Nakhon Ratchasima, Thailand*

[106]*Technical University of Košice, Košice, Slovak Republic*

[107]*The Henryk Niewodniczanski Institute of Nuclear Physics, Polish Academy of Sciences, Cracow, Poland*

[108]*The University of Texas at Austin, Austin, Texas, USA*

[109]*Universidad Autónoma de Sinaloa, Culiacán, Mexico*

[110]*Universidade de São Paulo (USP), São Paulo, Brazil*

[111]*Universidade Estadual de Campinas (UNICAMP), Campinas, Brazil*

[112]*Universidade Federal do ABC, Santo Andre, Brazil*

[113]*Universitatea Nationala de Stiinta si Tehnologie Politehnica Bucuresti, Bucharest, Romania*

[114]*University of Cape Town, Cape Town, South Africa*

[115]*University of Derby, Derby, United Kingdom*

[116]*University of Houston, Houston, Texas, USA*

[117]*University of Jyväskylä, Jyväskylä, Finland*

[118]*University of Kansas, Lawrence, Kansas, USA*

[119]*University of Liverpool, Liverpool, United Kingdom*

[120]*University of Science and Technology of China, Hefei, China*

[121]*University of South-Eastern Norway, Kongsberg, Norway*

[122]*University of Tennessee, Knoxville, Tennessee, USA*

[123]*University of the Witwatersrand, Johannesburg, South Africa*

[124]*University of Tokyo, Tokyo, Japan*

[125]*University of Tsukuba, Tsukuba, Japan*

[126]*Universität Münster, Institut für Kernphysik, Münster, Germany*

[127]*Université Clermont Auvergne, CNRS/IN2P3, LPC, Clermont-Ferrand, France*

[128]*Université de Lyon, CNRS/IN2P3, Institut de Physique des 2 Infinis de Lyon, Lyon, France*

[129]*Université de Strasbourg, CNRS, IPHC UMR 7178, F-67000 Strasbourg, France, Strasbourg, France*

[130]*Université Paris-Saclay, Centre d'Etudes de Saclay (CEA), IRFU, Départment de Physique Nucléaire (DPhN), Saclay, France*

[131]*Université Paris-Saclay, CNRS/IN2P3, IJCLab, Orsay, France*

[132]*Università degli Studi di Foggia, Foggia, Italy*

[133]*Università del Piemonte Orientale, Vercelli, Italy*

[134]*Università di Brescia, Brescia, Italy*

[135]*Variable Energy Cyclotron Centre, Homi Bhabha National Institute, Kolkata, India*

[136]*Warsaw University of Technology, Warsaw, Poland*

[137]*Wayne State University, Detroit, Michigan, USA*

[138]*Yale University, New Haven, Connecticut, USA*

[139]*Yonsei University, Seoul, Republic of Korea*

[140]*Zentrum für Technologie und Transfer (ZTT), Worms, Germany*

[141]*Affiliated with an institute covered by a cooperation agreement with CERN*

[142]*Affiliated with an international laboratory covered by a cooperation agreement with CERN*

[a]Also at Max-Planck-Institut fur Physik, Munich, Germany.

[b]Also at Italian National Agency for New Technologies, Energy, Sustainable Economic Development (ENEA), Bologna, Italy.

[c]Also at Dipartimento DET del Politecnico di Torino, Turin, Italy.

[d]Also at Yildiz Technical University, Istanbul, Türkiye.

[e]Deceased.

[f]Also at an institution covered by a cooperation agreement with CERN.

[g]Also at Department of Applied Physics, Aligarh Muslim University, Aligarh, India.

[h]Also at Institute of Theoretical Physics, University of Wroclaw, Poland.